AD-A175 673 TEMPERATURE DEPENDENCE OF IONIC ASSOCIATION AND OF MOLECULAR RELAXATION D (U) POLYTECHNIC UNIV FARMINGDALE NY WEBER RESEARCH INST N INOUE ET AL 1/1

UNCLASSIFIED NOV 86 TR-8 ARO-21758 6-CH DAAG29-85-K-0051 F/G 7/4 NL

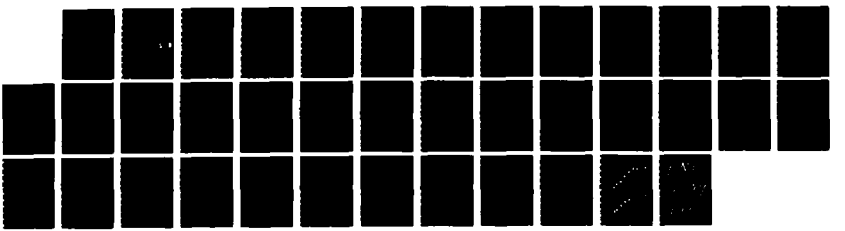

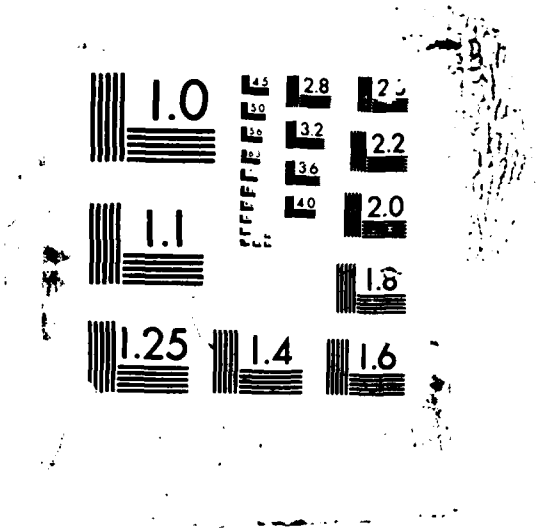
1.0
1.1
1.25
1.4
1.6
2.8
3.2
3.6
4.0
2.2
2.0
1.8

UNCLASSIFIED

SECURITY CLASSIFICATION OF THIS PAGE (When Data Entered)

REPORT DOCUMENTATION PAGE		READ INSTRUCTIONS BEFORE COMPLETING FORM
1. REPORT NUMBER ARO 21758.6-CH	2. GOVT ACCESSION NO. N/A	3. RECIPIENT'S CATALOG NUMBER N/A
4. TITLE (and Subtitle) Temperature Dependence of Ionic Association, and of Molecular Relaxation Dynamics of $LiAsF_6$ in 2-Methyletrahydrofuran		5. TYPE OF REPORT & PERIOD COVERED Technical 6. PERFORMING ORG. REPORT NUMBER 8
7. AUTHOR(s) Naoki Inoue, Meizhen Xu, and Sergio Petrucci		8. CONTRACT OR GRANT NUMBER(s) DAAG29-85-K-0051
9. PERFORMING ORGANIZATION NAME AND ADDRESS Polytechnic University Weber Research Institute Department of Chemistry Farmingdale, New York 11735		10. PROGRAM ELEMENT, PROJECT, TASK AREA & WORK UNIT NUMBERS N/A
11. CONTROLLING OFFICE NAME AND ADDRESS U. S. Army Research Office Post Office Box 12211 Research Triangle Park, NC 27709		12. REPORT DATE November 1986 13. NUMBER OF PAGES 34
14. MONITORING AGENCY NAME & ADDRESS(if different from Controlling Office)		15. SECURITY CLASS. (of this report) Unclassified 15a. DECLASSIFICATION/DOWNGRADING SCHEDULE

16. DISTRIBUTION STATEMENT (of this Report)

Approved for public release; distribution unlimited.

17. DISTRIBUTION STATEMENT (of the abstract entered in Block 20, if different from Report)

NA

18. SUPPLEMENTARY NOTES

The view, opinions, and/or findings contained in this report are those of the author(s) and should not be construed as an official Department of the Army position, policy, or decision, unless so designated by other documentation.

19. KEY WORDS (Continue on reverse side if necessary and identify by block number)

20. ABSTRACT (Continue on reverse side if necessary and identify by block number)

Electrical conductance data in the temperature range 25° to -35°C, analyzed by the Fuoss-Kraus triple-ions theory of conductance, reveal the presence of both ion pairs and triple ions. Evidence of the presence of the latter ones persists (with the formation constant K_T somewhat increased) even by allowing for measured changes of solvent permittivity with concentration of electrolyte. This dispenses any remaining doubt on the existence of triple ions. Formation constants K_P and K_T, at various temperatures for ion-pairs and

DD FORM 1 JAN 73 1473 EDITION OF 1 NOV 65 IS OBSOLETE

UNCLASSIFIED

SECURITY CLASSIFICATION OF THIS PAGE (When Data Entered)

20. ABSTRACT CONTINUED

triple ions respectively have been determined. These figures are compared with values calculated by the Bjerrum theory of ion-pairs formation and by the Delsignore-Bjerrum theory for formation of triple ions, respectively.

Ultrasonic relaxation spectra, in the concentration range 0.1M to 0.4M of $LiAsF_6$ and is the frequency range 0.5 to 400 MHz at 15° and 5°C in 2MeTHF, are reported. The results, combined with previous data at 25°C, are interpreted as due to ion-pair dimerization. The forward and reverse rate constants and activation parameters $\Delta H^{\neq}$ and $\Delta S^{\neq}$ are reported together with the values of the dimerization constants K_q at various T's. The figures for K_q are compared to the values calculated by the Maaser-Bjerrum dimerization theory of ion-pairs formation, giving pair to pair approach distances suggesting solvent separated dimers.

Infrared spectra in the ν_3 band envelope of the AsF_6^- ion, in the concentration range 0.05 to 0.8M, reveal the presence of three separated bands. The spectral envelope was deconvoluted by three Gaussian-Lorentzian product functions centered at ~716, ~702, and ~675 cm^{-1}. The band at ~702 cm^{-1} is interpreted as due to the "spectroscopically free" AsF_6^-, namely as due to solvent separated ion-pairs and/or solvent separated dimers. The band at ~716 cm^{-1} is interpreted as due to contact ion pairs, based on collateral evidence in 1,2 DME solvent. The band at ~675 cm^{-1}, according to literature evaluations of the AsF_6^- Raman and infrared spectra, is due to combination bands.

Temperature Dependence of Ionic Association, and of Molecular Relaxation Dynamics of $LiAsF_6$ in 2-Methyltetrahydrofuran

by

Naoki Inoue,* Meizhen Xu,** and Sergio Petrucci
Polytechnic University
Weber Research Institute
Department of Chemistry
Farmingdale, N.Y. 11735

ABSTRACT

Electrical conductance data in the temperature range 25° to −35°C, analyzed by the Fuoss-Kraus triple-ions theory of conductance, reveal the presence of both ion pairs and triple ions. Evidence of the presence of the latter ones persists (with the formation constant K_T somewhat increased) even by allowing for measured changes of solvent permittivity with concentration of electrolyte. This dispenses any remaining doubt on the existence of triple ions. Formation constants K_P and K_T, at various temperatures for ion-pairs and triple ions respectively have been determined. These figures are compared with values calculated by the Bjerrum theory of ion-pairs formation and by the Delsignore-Bjerrum theory for formation of triple ions, respectively.

Ultrasonic relaxation spectra, in the concentration range 0.1M to 0.4M of $LiAsF_6$ and is the frequency range 0.5 to 400 MHz at 15° and 5°C in 2MeTHF, are reported. The results, combined with previous data at 25°C, are interpreted as due to ion-pair dimerization. The forward and reverse rate constants and activation parameters $\Delta H^{\neq}$ and $\Delta S^{\neq}$ are reported together with the values of the dimerization constants K_q at various T's. The figures for K_q are compared

* On leave from the Department of Physics, Ehime University, Matsuyama, Japan.

** On leave from the Department of Chemistry, University of Peking, Peking, People's Republic of China.

to the values calculated by the Maaser-Bjerrum dimerization theory of ion-pairs formation, giving pair to pair approach distances suggesting solvent separated dimers.

Infrared spectra in the $\bar{\nu}_3$ band envelope of the AsF_6^- ion, in the concentration range 0.05 to 0.8M, reveal the presence of three separated bands. The spectral envelope was deconvoluted by three Gaussian-Lorentzian product functions centered at ~716, ~702, and ~675cm^{-1}. The band at ~702cm^{-1} is interpreted as due to the "spectroscopically free" AsF_6^-, namely as due to solvent separated ion-pairs and/or solvent separated dimers. The band at ~716cm^{-1} is interpreted as due to contact ion pairs, based on collateral evidence in 1,2-DME solvent. The band at ~675cm^{-1}, according to literature evaluations of the AsF_6^- Raman and infrared spectra, is due to combination bands.

Introduction

Knowledge of the extent of association of electrolyte solutions, and the type, structure and lifetime of the complex species in solutions used in secondary Li-battery construction, is a relevant information for electrochemists. The information becomes of paramount importance, in order to ascertain causes of battery failure when these units are subjected to low temperature as in stratospheric or subarctic conditions. On the other hand, theoretically, there is need of knowledge, but scarcity of data in the lifetime of complexes and in their structure in media of low permittivity. By changing temperature, the permittivity changes without concomitant large changes in donor number of solvent or other factors which occur in the usual isothermal studies in mixed solvents of various compositions. Therefore, in order to isolate electrostatic long range effects in ionic association of various species (without obscuring large changes of other factors), it appears that changing the temperature is an alluring way to perform these studies.

$LiAsF_6$ in 2 MeTHF, already studied at room temperature[1] has been now investigated by electrical conductance down to t=-35°C. Ultrasonic relaxation spectra have been produced at 15° and 5°C. In order to ascertain and confirm the structure of the $LiAsF_6$ in 2 MeTHF solvent, infrared spectra of the $\bar{\nu}_3$ band envelope of AsF_6^- are reported.

Experimental

The equipment and procedure for the conductance and ultrasonic work have been reported elsewhere.[1,2,3] Similarly, the equipment and procedure for the infrared work has been reported.[4] The only change is the computer assistance to the 983-G Perkin-Elmer spectrometer provided by a 3600 Perkin-Elmer data station that allows for spectra production, video monitoring, disc

recording and retrieving, data digitization and hard copy recording via computer. (The authors are indebted to the Perkin-Elmer staff of Norwalk Conn. for instruction of use of the 3600 data station).

For the products, $LiAsF_6$ was from Agri-Chemical Co., Atlanta, Ga. It was redried at 70°C in vacus for 36 hours. 2 MeTHF (Aldrich) was distilled under reduced pressure over metallic sodium and bentophenone. Solutions were used within 1 hour after preparation for the ultrasonic and infrared work minimizing (10-30 seconds) contact with the open atmosphere.

Solutions for conductance work were prepared by weight in situ, directly in the conductance cell, by adding a stock solution in weighed portions, to the weighed solvent in the cell. The stock solution, kept in a dessicator, was used within 6-8 hours from its preparation.

Results

Figs. 1A, B, and C report the equivalent conductances vs concentration, in the form $\log_{10}\Lambda$ vs. $\log_{10}c$, for $LiAsF_6$ in 2Methyltetrahydrofuran (2MeTHF) at 5°, -15°, and -35°C, respectively. Table I reports the experimental Λ's and c's for the various temperatures investigated.

Figs. 2A and B report representative plots of the excess sound absorption per wavelength $\mu = \alpha_{exc}\lambda = (\alpha - Bf^2)\frac{u}{f}$ where α is the attenuation coefficient (neper cm^{-1}) of sound at the frequency f. B is the background ratio, $B = (\alpha/f^2)_{f>>fr}$ for frequencies f's much larger than the relaxation frequency fr, $f >> fr$, in accord with the Debye function valid for a single relaxation process:

$$\frac{\alpha}{f^2} = \frac{A}{1+(f/fr)^2} + B. \qquad (I)$$

The solid lines in Figs. 2A and 2B are in fact, in accord to Eq. I, written in the

form:

$$\mu = 2\mu_m \frac{f/fr}{1+(f/fr)^2} \qquad (II)$$

where $\mu_m = \mu$ for f = fr; namely, the maximum excess sound absorption per wavelength, and $A = \frac{2\mu_m}{u\,fr}$; u is the sound velocity. Table II reports the calculated parameters fr, μ_m, B and the measured sound velocities u for all the solutions of $LiAsF_6$ in 2MeTHF investigated at 15°C and 5°C.

Figs. 3A and 3B show representative digitized infrared spectra of the $\bar{\nu}_3$ band envelope of the AsF_6^- ion. The solid lines have been drawn by fitting the digitized absorbances to the Gaussian-Lorentzian seimempirical product function:[4]

$$A = \sum_{j=1}^{3} A_j^\circ \left\{\exp\left[-\frac{(\bar{\nu}-\bar{\nu}_{oj})^2}{2\sigma_j^2}\right]\right\}\left[1+\frac{(\bar{\nu}-\bar{\nu}_{oj})^2}{\sigma^2}\right]^{-1} \qquad (III)$$

where the $\left[\exp-\frac{(\bar{\nu}-\bar{\nu}_{oj})}{2\sigma_j^2}\right]$ is the Gaussian, and $\left[1+\frac{(\bar{\nu}-\bar{\nu}_{oj})^2}{\sigma^2}\right]^{-1}$ the Lorentzian factor of III. σ_j^2 is the variance and, $\sigma_j = \left[\frac{\Delta\bar{\nu}_{1/2}}{1.46}\right]$ with $\Delta\bar{\nu}_{1/2}$ the width of each band and at half maximum absorbance $A_j^\circ/2$. A_j° corresponds to the maximum absorbance for $\bar{\nu} = \bar{\nu}_{oj}^\circ$ for each band. Notice that for a pure Gaussian function $A = A_j^\circ\exp\left[-\frac{(\bar{\nu}-\bar{\nu}_{oj})^2}{2\sigma_j^2}\right]$, $\sigma = \frac{\Delta\bar{\nu}_{1/2}}{2.355}$, whereas for a pure Lorentzian $A = A_j^\circ\left[1+\frac{(\bar{\nu}-\bar{\nu}_{oj})^2}{2\sigma_j^2}\right]^{-1}$, $\sigma = \frac{\Delta\bar{\nu}_{1/2}}{2.00}$. The factors 2.355 and 2.00 relate the half bandwiths of the respective functions to the standard error σ. For instance, for a pure Gaussian $0.50 = f(x) = \frac{A}{A_o} = e^{-(\bar{\nu}-\bar{\nu}_o)^2/2\sigma^2} =$

$\exp(-\frac{\Delta\bar{\nu}_{1/2}^2/4}{2\sigma^2})$, giving $2.3548 = \frac{\Delta\bar{\nu}_{1/2}}{\sigma}$. As a pure Gaussian function is particularly appropriate for infrared spectrum of solids and a pure Lorentzian is appropriate for infrared spectra of gases, the product function III is an average function, attempting empirically, but quite successfully at reproducing the line shape of infrared spectra in the liquid state. Table III reports the calculated parameters $A_{oj}, \bar{\nu}_j, \Delta\bar{\nu}_{1/2}$ for the three Gaussian-Lorentzian product functions used to describe the $\bar{\nu}_3$ band envelope of $LiAsF_6$ in 2MeTHF.

Calculations and Discussion

a) Electrical conductivity

D'Aignaux et al.[1] reported conductance data for $LiAsF_6$ in 2MeTHF at 25°C. Some of their data have been reanalyzed by the Fuoss Kraus triple ion conductance theory:[5]

$$\Lambda g(c)\sqrt{c} = \frac{\Lambda_o}{\sqrt{K_p}} + \frac{\Lambda_T^o K_T}{\sqrt{K_p}}\left(1 - \frac{\Lambda}{\Lambda_o}\right)c\,, \qquad \text{(IV)}$$

with

$$g(c) = \frac{\exp\left(-\frac{2.303}{\Lambda_o^{1/2}}\beta'\sqrt{c\Lambda}\right)}{\left(1 - \frac{S}{\Lambda_o^{3/2}}\sqrt{c\Lambda}\right)\left(1 - \frac{\Lambda}{\Lambda_o}\right)^{1/2}},$$

and

$$\beta' = \frac{1.8247 \times 10^6}{(\epsilon T)^{3/2}}\,;\; S = \alpha\Lambda_o + \beta = \frac{0.8206 \times 10^6}{(\epsilon T)^{3/2}} + \frac{82.501}{\eta(\epsilon T)^{1/2}}\,.$$

On the above, ϵ is the permittivity, η the viscosity and T the absolute temperature. The value of $\epsilon = 6.24$ and $\eta = 0.0047$ p have been taken from previous

work.[1] The value $\Lambda^\circ = 22.53\ \Omega^{-1}cm^2eq^{-1}$ at t = 25.00C, in propylene carbonate,[7] is judged particularly reliable. As $\eta = 0.0253P$[7] it gives $\Lambda_o\eta = 0.570$ and, in 2MeTHF, $\Lambda^\circ = 121\Omega^{-1}cm^2eq^{-1}$, lower than the value used previously,[1] and the very reason of re-analyzing the data.

Fig. 4A reports the plot of $\Lambda g(c)\sqrt{c}$ vs. $\left(1-\frac{\Lambda}{\Lambda_o}\right)c$ for $LiAsF_6$ in 2MeTHF. Lineary regression gives $r^2 = 0.997$, intercept I = - 0.02447, Slope = 0.4793, from which one calculates $K_p = 2.4_5 \times 10^7 M^{-1}$ and $K_T = 29.4$ having retained the arbitrary condition $\Lambda^\circ_T = \frac{2}{3}\Lambda_o$, consistent with previous work.[1]

Recently,[7] it has been inferred that because the permittivity of the electrolyte solution increases with concentration of electrolyte, the deviation of the slope of $\log_{10}\Lambda$ *vs.* $\log_{10}c$ from -0.50, namely from the Ostwald mass law, may be due in part or all to changes in permittivity, thereby putting the very existence of triple ions under discussion. We agree that, at high concentrations, the permittivity effect becomes of paramount importance, as documented in a previous paper.[9] We were concerned, however, that even at low concentration $c \leq 2 \times 10^{-2} M$ the fact that $\epsilon(c)$ is larger than the solvent value may be significant.

We therefore took the Delsignore et al.[1] data of dielectric permittivity ϵ for $LiAsF_6$ in 2MeTHF, and fitted them by nonlinear regression to the equation at t=25°c

$$\epsilon = 6.24 + 47.34c - 242.77c^2$$

with determination coefficient $r^2 = 0.999999_7$ (Fig. 4B). At each concentration used in the conductance work, ϵ was then calculated and Eq. IV applied, (Fig. 4C). Linear regression of $\Lambda g(c)\sqrt{c}$ *vs.* $\left(1-\frac{\Lambda}{\Lambda_o}\right)c$ gives

$r^2 = 0.9965$, $I = 0.02430$, $S = 0.5874$ from which $K_p = 2.48 \times 10^7 m^{-1}$ and $K_T = 36._2 M^{-1}$, having used equation IV up to $c = 0.02155$. The change in K_p is insignificant, with respect to the calculation of K_p with $\epsilon = 6.24$, the solvent value. The change in K_T is about 20%, but but using $\epsilon = \epsilon(c)$ does not causes K_T to become zero, as the allegation involving $\epsilon(c) > \epsilon_{solvent}$ may have implied. As the condition $\Lambda_T^\circ = \frac{2}{3}\Lambda_o$ probably carries an incertitude at least as large as 20%, in what follows we shall use the value of $K_T = 29M^{-1}$ to compare internally and relatively its change with temperature. Table IV reports the results of the calculations by the Fuoss-Kraus conductance Eq. IV at 5°C – 15°C and – 35°C. For these calculations the permittivities ϵ and viscosities η have been calculated by the functions

$$\epsilon = -1.14 + \frac{2200}{T} \ ,$$

$$\log_{10}\eta = -3.635 + \frac{386}{T} \ .$$

Table IV reports also, for all the temperatures investigated the maximum concentration used in Eq. IV. Fig. 5A reports the Van't Hoff plot of ℓnK_p vs. $1/T$ for $LiAsF_6$ in 2MeTHF. Fig. 5B reports the corresponding Van't Hoff plot of ℓnK_T vs. $1/T$ for the same system.

The solid lines, calculated by linear regression, give: from Fig. 5A $\Delta S_p^\circ = 63$ cal/Kmol, $\Delta H_p^\circ = 7.28 \frac{Kcal}{mol}$. By equating K_p to the Bjerrum expression for ion-pair association:[10]

$$K_{Bj} = \frac{4\pi L d^3}{1000} \beta^3 Q \qquad (V)$$

where

$$\beta = e^2/\epsilon dkT \ , \quad Q = \int_2^\beta \frac{e^Y}{Y^4} dY$$

one obtains the values of d, the ion-pair separation distance reported in Table V. The value at t=25°c is in good accord with the value $d_\mu = 4.6 \times 10^{-8}$cm, calculated[1] from the Böttcher function[11] and dielectric permittivities. There appears to be a trend, d increasing by decreasing temperature. If true, this trend would suggest a tendency to form solvent separated ion-pairs by decreasing T(hence by increasing ϵ).

The triple ions formation constants K_T have been compared to the Delsignore-Bjerrum[12] equilibrium constant:

$$K_{BjT} = \frac{2\pi L a_T^3}{1000} b_T^{3/2} Q_T \qquad (VI)$$

with

$$b_T = \frac{e\mu}{\epsilon a_T^2 kT} \; ; \; Q = \sum_{n=odd} \left| \frac{Y^{(n-5/2)}}{(n-(5/2))n!} \right|_{Y=2}^{Y=b_T} \text{ or}$$

$$Q = -\frac{b_T^{-1.5}}{1.5} + \frac{b_T^{0.5}}{(0.5)3!} + \frac{b_T^{2.5}}{(2.5)5!} + \frac{b_T^{4.5}}{(4.5)7!} + \frac{b_T^{6.5}}{(6.5)x9!}$$

$$+ \frac{b_T^{8.5}}{(8.5)11!} + \ldots - 0.2556$$

using the experimental[1] $\mu = 22 \times 10^{-18}$ esu cm.

The results extending the series to n= 15 are reported in Table V. At t=25°C, $a_T = 8.4 \times 10^{-8}$cm; namely, a_T larger than 1.5d. (The axiom of three equal spheres at contact may suggest $a_T = 1.5\,d$.) The values of a_T seem however of reasonable magnitude, even at the lowest temperature, with the general condition $a_T \approx 2d$. In Table V the Delsignore-Bjerrum parameters[12] q_T are also reported showing a_T approaching q_T (hence K_T approaching zero) as the temperature is lowered (hence, as ϵ is increased). In the above $q_T = \left(\frac{1}{2}\frac{e\mu}{\epsilon kT}\right)^{1/2}$

which corresponds to a ration of 2 between the electrostatic ion dipole energy $\frac{e\mu}{\epsilon q_T^2}$ and kT.

b) Ultrasonic relaxation spectra

Delsignore et.al.[1] interpreted the observed ultrasonic relaxation of $LiAsF_6$ in 2MeTHF at t = 25°C as due to a dimerization process according to the scheme:

$$2LiAsF_6 \underset{k_r}{\overset{k_f}{\rightleftharpoons}} (LiAsF_6)_2, \qquad \text{(VII)}$$

leading to the relation

$$\tau^{-1} = 2\pi f_r = 4k_f c_p + k_r, \qquad \text{(VIII)}$$

with $K_q = k_f/kr$. By approximating $c_p \approx c$, namely the ion-pair concentration to the total concentration, and by plotting τ^{-1} vs. c, k_f,k_r and hence K_q could be calculated.

Figs. 6A and 6B report such a plot. Specifically, at 15°C, linear regression gives $r^2 = 0.96$, Int = 1.38×10^8 and Slope = $7.9_7 \times 10^8$. At 5°C linear regression gives $r^2 = 0.85$ Int

In Table VI the values of k_f,k_r,K_q at 25°C, taken from previous work,[1] and at 15°C and 5°C, taken from the present data, are reported.

Figs. 7A and 7B report the Eyring plots of $\ell n(k_f/T)$ and $\ell n\ (k_r/T)$ vs. 1/T, respectively. The solid lines have been calculated by linear regression. Specifically, one obtains from the data of Fig. 7A,

$$r^2 = 0.999\ , \qquad I = 21.9\ , \qquad S = -2437$$

giving

$$\Delta H_f^{\neq} = 4.8_4 \text{ Kcal/mol}, \qquad \Delta S_f^{\neq} - 3.7_0 \text{ cal/Kmol}.$$

Also one obtains from the data of Fig. 7B,

$$r^2 = 0.956 \ , \qquad I = 15.2_7 \ , \qquad S = -637._4 ,$$

giving

$$\Delta H_f^{\neq} = 1.2_7 \text{ Kcal/Kmol} \ , \qquad \Delta S_f^{\neq} = -16.8_7 \text{ cal/Kmol} .$$

Therefore,

$$\Delta H_q^{\circ} = \Delta H_f^{\neq} - \Delta H_r^{\neq} = 3.6 \text{Kcal/mol},$$

and

$$\Delta S_q^{\circ} = \Delta S_f^{\neq} - \Delta S_r^{\neq} = 13._2 \text{ cal/Kmol},$$

giving at T = 298.2:

$$\Delta G_q^{\circ} = 3{,}600 - 298\ (13.2) = -336._2 \text{ cal/mol}$$

and $K_q = \exp\left(\dfrac{336._2}{1.987 \times 298.2}\right) = 1.7_6 \ M^{-1}$,

remarkably close to the value obtained before from the isothermal work at 25°C

It was of interest, at this point, to compare the experimental K_q from Table VI to theoretical values.

For this purpose we have used the Maaser-Bjerrum theory[13] which reads:

$$K_{Bjq} = \frac{4\pi L a_q^3}{3000} \, b_q \, Q_q \qquad \text{(IX)}$$

with

$$b_q = \frac{\mu^2}{\epsilon a_q^3 kT} \ , \text{ and}$$

$$Q_q = 0.6667 - \frac{1}{b_q} + \sum_{n_{odd}} \frac{1}{(n+2)!n} [b_q^n - (1.5)^n]$$

for all odd n's (n = 1,3,5...).

By extending the summation to n = 25, we have calculated K_{Bjq} by varying a_q in steps of 0.1°A to match with the experimental K_q's.

Table VI reports the calculated K_q's and the corresponding a_q's. A small trend seems to exist; the a_q's slightly increasing by decreasing T (as noticed for the a_T's, above). Further, at t = 25°C, $a_q = 9.4 \times 10^{-8}$cm $\simeq 2$ d where d = 4.6×10^{-8}cm. This implies that the two dipoles are separated more from each other than the two ions in the pair, or in other words it implies a solvent separated dimer.

c) Infrared Spectra

The Raman and infrared spectra of AsF_6^- in the solid state have been discussed in the literature.[14] The assignment of the fundamental vibrational frequencies has been done on the assumption of an octahedral O_h structure for AsF_6^-.

Three Raman-active fundamental vibrations, $\bar{\nu}_1(A_{1g}) \cong 685$ cm^{-1}, $\bar{\nu}_2(E_g) = 576$ cm^{-1} doubly degenerate, and $\bar{\nu}_5(F_{2g}) = 372$ cm^{-1}, were observed.[14] Two infrared active vibrations $\bar{\nu}_3(F_{1u}) \cong 699$ cm^{-1} and $\bar{\nu}_4(F_{1u}) \cong 392$ cm^{-1}, both triply degenerate, were also observed. The sixth vibration $\bar{\nu}_6$ was reported as inactive in both Raman and infrared spectra.[14] The vibrational mode of frequency $\bar{\nu}_6$, which is inactive in the O_h structure, was predicted to become infrared active in all the lower symmetries with expected frequencies in the 200-400 cm^{-1} range. In fact, the position of the $\bar{\nu}_6$ band was estimated[14] to be $\bar{\nu}_6 = 322$ cm^{-1} for AsF_6^-, a calculation based on force constants estimations. It is worth quoting[14] that the two combination bands

($\bar{\nu}_5 + \bar{\nu}_6$) and ($\bar{\nu}_2 + \bar{\nu}_6$) were expected to be active in the infrared band of these compounds. In fact, shoulders in the infrared spectra were observed[14] in the region of the $\bar{\nu}_3$ band. (Notice, in fact, that $\bar{\nu}_2 + \bar{\nu}_6 \sim 372 + 322^- = {}^-694\ cm^{-1}$, closely overlaps the $\bar{\nu}_3$ band, an observation to be quoted again below.)

We have chosen the $\bar{\nu}_3$ infrared band region for our study, as reported above in Table III. In view of the literature,[14] the band at 702 cm^{-1} can then be assigned to the "spectroscopically free" AsF_6^-; namely (in view of the conductance results, giving $K_p \cong 10^7 M^{-1}$), to a solvent separated ion-pair Li^+S,AsF_6^-, and possibly to smaller amounts of solvent separated dimers $(Li^+S,AsF_6^-)_2$, spectroscopically indistinguishable from Li^+S,AsF_6^- . The band at $\approx$717 cm^{-1} appears to change in maximum absorbance with the nature of the solvent. This is testified in the spectra reported in Fig. 8A for $LiAsF_6$ in 1,2-DME of permittivity $\epsilon = 7.0$, and in Fig. 8B for $LiAsF_6$ in THF of permittivity $\epsilon = 7.4$ (both ϵ's referring to T = 298.2K). Further, in Fig. 9B, $LiAsF_6$ in acetone shows that the band at 718 cm^{-1} is of minor relative maximum absorption A_o, and only necessary to describe the left "wing" of the $\bar{\nu}_3$ band of the AsF_6^- spectrum, which cannot be reproduced by a single Gaussian-Lorentzian band (Fig. 9A). Acetone (dried over molecular sieves, distilled and checked for absence of water bands at $\approx$3600 cm^{-1}) has a permittivity $\epsilon = 20.5$ at T = 298.2K. Further, in 2MeTHF, the value of A_o^{717} increases with respect to A_o^{702}, surpassing it at about c = 0.3M (Table III). We assign this band at $\bar{\nu} \cong 717\ cm^{-1}$ to a contact species, which is favored by either decreasing the permittivity of the solvent, or by increasing the electrolyte concentration (by mass law).

Previous ultrasonic work, for $LiAsF_6$ in 1,2 DME[15] did not reveal presence of dimers, but only presence of an outer sphere to contact ion-pair equilibrium:

$$L^+S,AsF_6^- \rightleftarrows LiAsF_6 + S$$

strongly shifted toward the left. Raman spectra[15] confirmed this assignment, the $\bar{\nu}_1(A_{1g})$ band, at $\approx$680 cm^{-1}, being almost without either discernible band asymmetry or satellite bands present.

Similarity of the infrared bands positions in 1,2 DME at about 717 cm^{-1}, 702 cm^{-1} and 677 cm^{-1} with the ones of $LiAsF_6$ in 2MeTHF, suggest that the origin of these three bands is the same. This leads toward assignment of the 717 cm^{-1} band to contact ion-pairs, $LiAsF_6$. Probably the contact ion-pairs are in much larger relative concentration in 2MeTHF with respect to 1,2-DME, judging from the relative band amplitudes at $\approx$ 717 cm^{-1}. By the same argument, in acetone (Figs. 9A and 9B), these contact species are almost absent. This is in accord to expectations due to the permittivities of the three solvents.

The interpretation of the band at $\approx$676 cm^{-1} can be achieved by assigning this band as due to a combination band[14] $(\bar{\nu}_2 + \bar{\nu}_6)$, $\bar{\nu}_6$ being present when the O_h symmetry is lowered because of the formation of contact species. Fig. 10 shows the $\bar{\nu}_3$ region of the infrared spectrum of $LiAsF_6$ in Dimethylcarbonate (DMC), a solvent of permittivity $\epsilon = 3.1$.[8] The spectrum looks qualitatively similar to the one in 1,2 MeTHF at similar concentrations. Notice that the band at 676 cm^{-1} is practically invisible for the spectrum of $LiAsF_6$ in acetone (Fig. 9), where only a minuscle band contribution at $\bar{\nu}$ = 682 cm^{-1} is needed in order to describe the lower "wing" of the spectrum. On the other hand, for $LiAsF_6$ in DMC, dimers were found to be present,[8] with an apparent formation constant $K_q \cong 50\ M^{-1}$. One could then argue that lowering of the O_h symmetry of AsF_6^-, is also due to some contact dimers, contributing to the band at $\bar{\nu} \cong 676\ cm^{-1}$. This band appears to be present in different but increasing relative amplitudes in THF, 1,2-DME, 2MeTHF and in DMC. In acetone the satellite bands at 717 and 628 cm^{-1} are almost absent. Energetically, dimers

should not be stable configurations in acetone, the dipole-dipole energy being small with respect to kT, due to the permittivity $\epsilon = 20.5$ at $T = 298.2K$.

Lack of visibility of the dimers in the infrared spectrum of $LiAsF_6$ in 2 MeTHF, despite their formation constants $K_q = 1.8\ M^{-1}$ at 25°C, may be rationalized if they are in the majority of the outer-sphere or solvent separated type. This was suggested by theoretical calculations above, indicating $a_q = 9.4 \times 10^{-8}cm \cong 2d$, d being the ion-pair separation distance. Because of the likely contribution of both species, LiS,AsF_6 and $(Li^+S,AsF_6)_2$ to the band at $\bar{\nu} = 702\ cm^{-1}$, we believe that any attempt at calculating formation constants from the absorbances of the two visible bands at 702 cm^{-1} and 717 cm^{-1}, may lead to meaningless results.

In order to facilitate calculations from the present data, as reported in Table III, we have expressed the absorbances per unit length A_o^{717}/ℓ, A_o^{702}/ℓ and $A_o^{676}\ell$ by polynomials in the electrolyte concentration $c(mol/dm^3)$. Specifically, nonlinear regression gives:

$$A_o^{717}/\ell = -1.1 + 863\ c + 832\ c^2 - 1384\ c^3\ ,\text{with } r^2 = 0.994;$$

$$A_o^{702}/\ell = -1.5 + 1199\ c - 1006\ c^2 + 239.5\ c^3,\ \text{with } r^2 = 0.997;$$

$$A_o^{676}/\ell = 0.062 + 2006.4\ c + 233.9\ c^2 - 241.5\ c^3,\text{with } r^2 = 0.996,$$

having given 50% statistical weight to the origin.

Acknowledgment

This work was supported by the Army Office for Scientific Research, Durham, North Carolina, under Grant No. DAAG-29-85-K0048. Thanks are expressed for their generous support.

Table I

Equivalent conductance ($\Omega^{-1}cm^2eq^{-1}$)Λ and molar concentration c(mol/dm^3) at t = 25°, 5°, – 15° and – 35°C for $LiAsF_6$ in 2MeTHF.

t = 25°C[a]		t = 5°C	
Λ	c x 10^4	Λ	c x 10^4
		1st Run	
1.037_1	6.6112	4.966_5	5.7974
0.894_5	9.5847	3.431_6	13.949
0.498_4	38.470	2.680_5	28.308
0.416_5	62.710	2.070_0	67.019
0.372_1	89.505	1.738_9	141.95
0.332_1	140.42	1.538_1	397.93
0.315_8	215.55	1.577_4	723.66
0.338_6	353.00	1.654_9	924.71
		2nd Run	
		1.551_9	583.3
		1.654_3	832.8
		1.828_1	1180.0
		2.475_3	2493.1

t = – 15°C		t = – 35°C	
Λ	c x 10^4	Λ	c x 10^4
1st Run		1st Run	
4.255_5	5.2038	5.5235	5.5345
2.6909	18.282	3.9513	13.358
2.0330	38.389	3.0785	27.699
1.3753	112.73	2.4651	55.844
1.0609	251.86	1.8774	130.17
0.9849_5	425.65	1.4546	274.37
1.0513	706.70	1.2912	498.81
1.2334	1132.1	1.2577	780.85
		1.3492	972.82
2nd Run		2nd Run	
1.4487	1628.3	1.5649	1318.6
1.8250	2592.6	1.9144	2611.8

[a] Data from Ref. 1

Table II

Ultrasonic relaxation parameters fr, μ_m, B and sound velocities u for $LiAsF_6$ in 2MeTHF at the concentrations and temperatures investigated.

c (mol/dm^3)	fr (MHz)	$\mu_m \times 10^5$ --	$B \times 10^{17}$ ($cm^{-1}s^2$)	$u \times 10^{-5}$ ($cm\,s^{-1}$)
t = 15°C				
0.40	70	570	62	1.249
0.30	65	530	52	1.245
0.20_1	45	500	56	1.259
0.10_5	50	350	55	1.258
t = 5°C				
0.40_6	60	670	50	1.296
0.30	40	600	50	1.300
0.20	40	410	50	1.276
0.10_6	30	270	46	1.285

Table III

Calculated infrared parameters A_{oj}, $\bar{\nu}_j$ and $(\Delta\nu_{1/2})$ for the concentrations investigated of $LiAsF_6$ in 2MeTHF.

ℓ_{cell} (cm)	c (mol/dm^3)	$\bar{\nu}_{717}$ (cm^{-1})	A_o^{717} --	$\bar{\nu}_{702}$ (cm^{-1})	A_o^{702} --	$\bar{\nu}_{675}$ (cm^{-1})	A_o^{675} --	$\Delta\nu_{1/2}$[a] (cm^{-1})
0.00259	0.803	717.5	1.35	702	1.15	676	0.50	13
0.00258	0.601	717.5	1.25	702	1.00	676	0.40	12
0.00270	0.502	717	1.32	702	1.05	676	0.36	12
0.00268	0.402	717	1.11	702	0.92	676	0.29	12
0.00270	0.302	717	0.83	702	0.78	675	0.22	12
0.00504	0.210	716	0.85	702	1.00	675	0.20	12
0.00496	0.106	717	0.55	702.5	0.50	676	0.17	12
0.00468	0.053	716	0.17_2	702.5	0.25_6	675	0.04	12

[a] $(\Delta\nu_{1/2})_{717} = (\Delta\nu_{1/2})_{702} = (\Delta\nu_{1/2})_{675}$

Table IV

Solvent properties and results of K_p and K_T by the Fuoss-Kraus triple-ions conductance equation for $LiAsF_6$ in 2MeTHF at the various temperatures investigated.

t (°C)	ϵ --	η (poise)	Λ_o[1] ($\Omega^{-1}cm^2eq^{-1}$)	K_p (M^{-1})	K_T[2] (M^{-1})	C_{rmax}[3] x10^4
25	6.24	0.0047	121	$2.5x10^7$	29.4	215.5_5
5	6.77	0.0057	100	$1.0x10^6$	$20._3$	141.9_5
-15	7.38	0.0072_5	$78._6$	$8.5x10^5$	$9._8$	112.7_3
-35	8.10	0.0096_8	$58._9$	$3.0x10^5$	$1._3$	130.1_7

[1] based on Walden's rule $\Lambda_o\eta = 0.570$
[2] based on the arbitrary position $\Lambda_o^T = 2/3\Lambda_o$
[3] maximum electrolyte concentration used in Eq. IV

Table V

Calculated ion-pair separation distance d and triple ion separation distance a_T, according to the Bjerrum and Delsignore-Bjerrum theories, respectively, for $LiAsF_6$ in 2MeTHF at various temperatures. Values of q_T, the maximum distance of separation of an ion from the dipole pair in the triple ion.

t (°C)	K_p^{exp} (M^{-1})	K_p^{calc} (M^{-1})	K_T^{exp} (M^{-1})	K_T^{calc} (cm)	$dx10^8$ (cm)	a_Tx10^8 (cm)	q_Tx10^8
25	$2.5x10^7$	$2.4x10^7$	29.4	30.0	4.5	8.4	14.34
5	$1.0x10^6$	$1.1x10^6$	$20._3$	20.0	5.5	9.2	14.25
-15	$8.5x10^5$	$9.0x10^5$	$9._8$	$9._7$	5.5	11.0	14.27
-35	$3.0x10^5$	$3.0x10^5$	$1._3$	$1._3$	6.0	13.6	14.08

† The calculated K_p^{calc} and K_T^{calc} have been computed from Eqs. V and VI respectively by changing d and a_T in steps of $0.1x10^{-8}$cm.

Table VI

Values of the rate constants and equilibrium constants at various temperatures for the dimerization of Li AsF_6 in 2MeTHF. Calculated values of K_q and a_q according to the Maaser-Bjerrum theory of dimerization.

(°C)	k_f $M^{-1}(s^{-1})$	k_r (s^{-1})	K_q (M^{-1})	$K_q^{calc\dagger}$ (M^{-1})	$a_q x10^8$ (cm)
25	$2.7x10^{8\ddagger\ddagger}$	$1.5x10^{8\ddagger\ddagger}$	$1.8^{\ddagger\ddagger}$	1.80	9.4
15	$2.0x10^8$	$1.4x10^8$	1.4	1.36	9.7
5	$1.4x10^8$	$1.2x10^8$	1.2	1.19	9.8

†The calculated K_q^{calc} have been computed from Eq. IX by changing a_q in steps of $0.1x10^{-8}$cm.

‡‡Figure taken from reference 1.

REFERENCES

1. Delsignore M., Maaser H.E., Petrucci, J. Phys. Chem. (1984) 88, 2405.
2. Petrucci S., Hemmes P., Battistini M, J. Am. Chem. Soc. (1967), 89, 5582.
3. Darbari G.S., Richelson M., Petrucci S., J. Chem. Phys. (1970), 53, 859; Petrucci S. J. Phys. Chem. (1967) 71, 1174; Onishi S. Farber H., Petrucci S., J. Phys. Chem. (1980) 84, 2922.
4. Saar D. Petrucci S., J. Phys. Chem. (1986) 90, 3326.
5. Fuoss R.M., Kraus C.A., J. Am. Chem. Soc. (1933), 55, 2387 Fuoss R.M., Accascina F., Electrolytic Conductance Intersci. N.Y. (1959).
6. Salomon M., Plichta E.J., Electrochim Acta (1984), 29, 731.
7. Gestblom B., Svorstöl I., Songstad J., J. Phys. Chem. (1986), 90, 4684.
8. Delsignore M., Farber H., Petrucci S., J. Phys. Chem. (1985) 84, 4968.
9. Nicholls D., Sutphen C., Szwarc M., J. Phys. Chem. (1968) 72, 1021.
10. Bjerrum N.K. Dan Vidensk Selsk. Mat.-Fys. Medd (1926) 7, 9.
11. Böttcher C.F.J., Theory of Electrical Polarizaiton Elsevier, Amsterdam 1973.
12. Delsignore M., Farber H., Petrucci, S., J. Phys. Chem. (1986) 90 66; ibid (1986) 90, 3294.
13. Maaser H.E., Delsignore M., Newstein M., Petrucci S. J. Phys. Chem. (1984) 88 5100.
14. Begun G.M., Rutenberg A.C., Inorg-Chem. (1967) 12, 2212.
15. Farber H., Petrucci S., J. Phys. Chem. (1983) 87, 3515.

List of Figures

Fig. 8 (A) Infrared spectrum of $LiAsF_6$ in 1, 2 Dimethoxyethane (DME) ($\overline{\nu}_3$ infrared envelope).

(B) Infrared spectrum of $LiAsF_6$ in Tetrahydrofuran (THF) ($\overline{\nu}_3$ infrared envelope). The broad band at $\sim$660 cm^{-1} is a solvent band.

Fig. 9 (A) Digitized infrared spectrum of $LiAsF_6$ 0.20M in acetone ($\overline{\nu}_3$ region). Dashed line---single Gaussian-Lorentzian band.

(B) Digitized infrared spectrum of $LiAsF_6$ 0.20M in acetone. Solid line, sum of three Gaussian-Lorentzian bands.

Fig. 10 Infrared $\overline{\nu}_3$ band envelope of $LiAsF_6$ 0.20M in Dimethylcarbonate.

Fig. 11 (A) Maximum absorbance per unit length (A_o^{717}/ℓ) vs. concentration c of $LiAsF_6$ in 2MeTHF.

(B) Maximum absorbance per unit length (A_o^{707}/ℓ) vs. concentration of electrolyte $LiAsF_6$ in 2MeTHF.

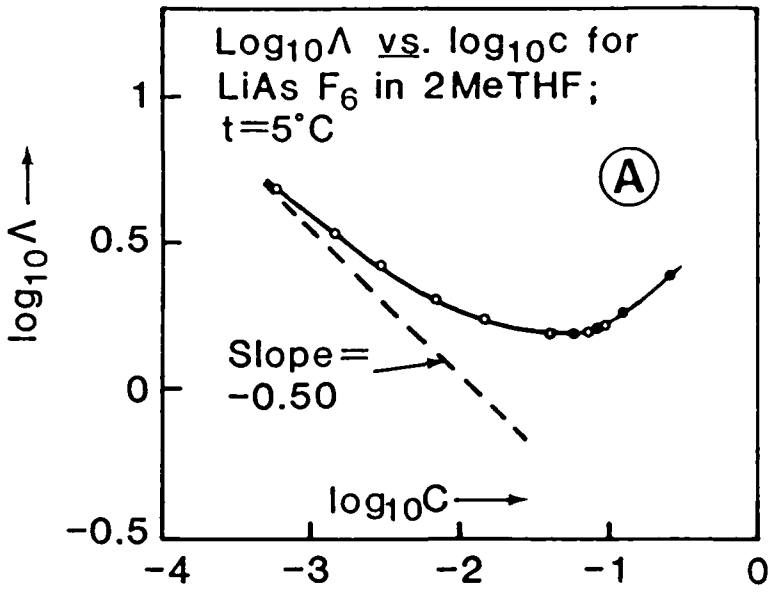
Log10Λ vs. log10c for
LiAs F6 in 2MeTHF;
t=5°C
A
Slope=
-0.50
log10Λ
log10C
1
0.5
0
-0.5
-4
-3
-2
-1
0

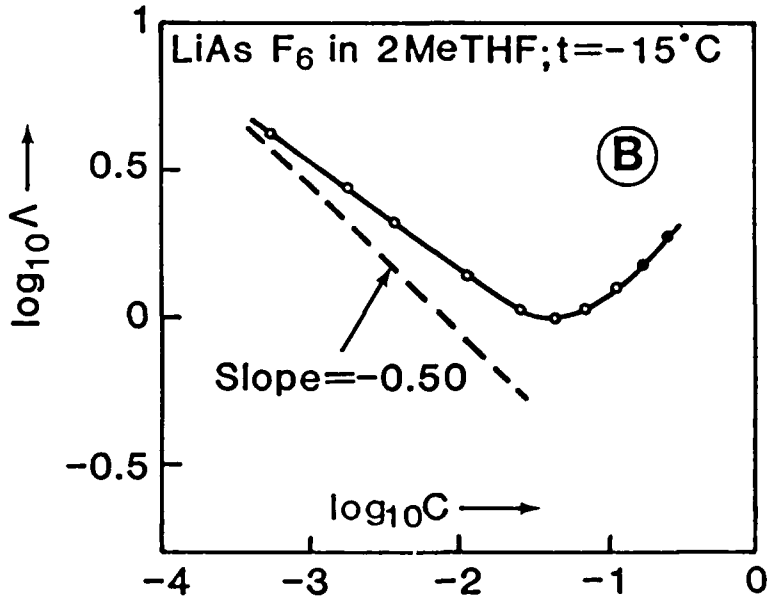
LiAs F6 in 2MeTHF;t=-15°C
B
Slope=-0.50
log10Λ
log10C
1
0.5
0
-0.5
-4
-3
-2
-1
0

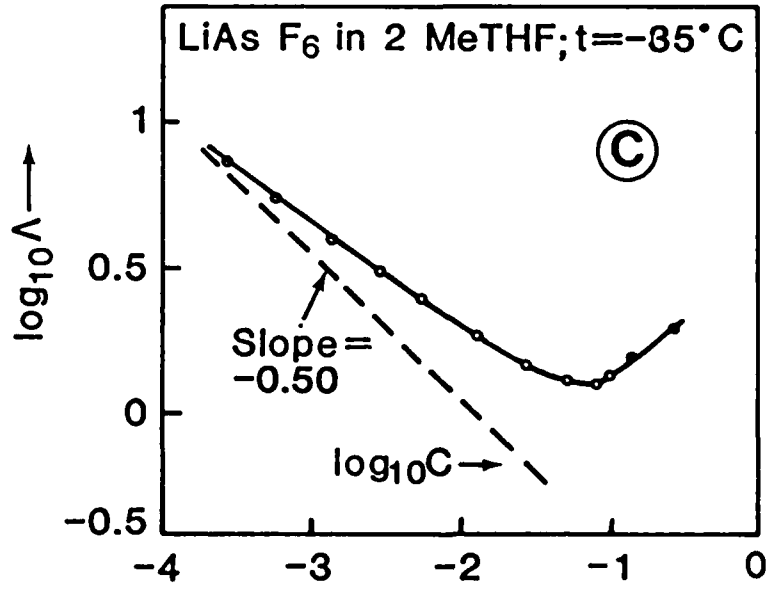
LiAs F6 in 2 MeTHF;t=-35°C
C
Slope=
-0.50
log10Λ
log10C
1
0.5
0
-0.5
-4
-3
-2
-1
0

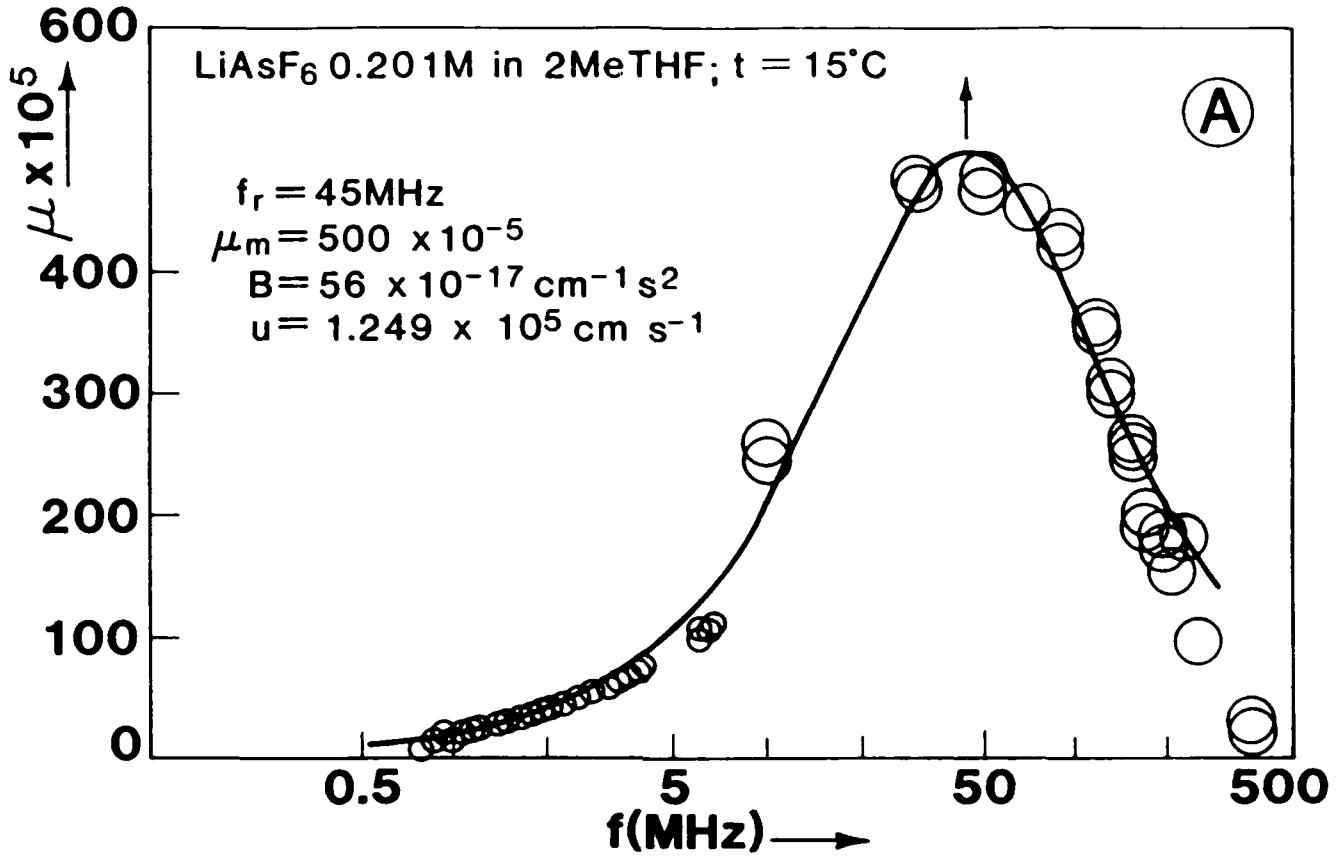
LiAsF6 0.201M in 2MeTHF; t = 15°C
A
fr = 45MHz
μm = 500 x10-5
B = 56 x10-17 cm-1 s2
u = 1.249 x 105 cm s-1
μ x10^5
600
400
300
200
100
0
0.5
5
50
500
f(MHz)

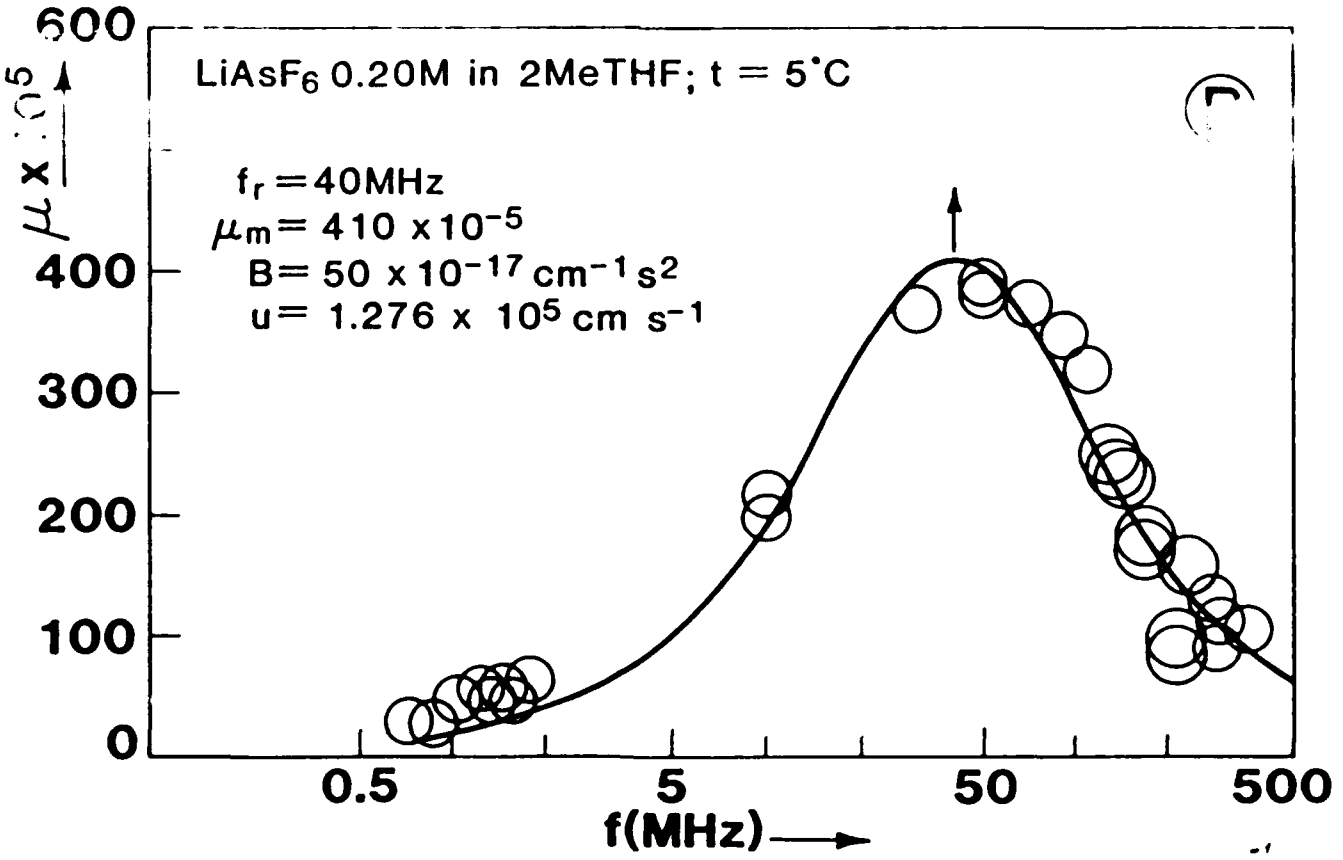
LiAsF6 0.20M in 2MeTHF; t = 5°C
fr = 40MHz
μm = 410 x10-5
B = 50 x10-17 cm-1 s2
u = 1.276 x 105 cm s-1
600
400
300
200
100
0
0.5
5
50
500
f(MHz)

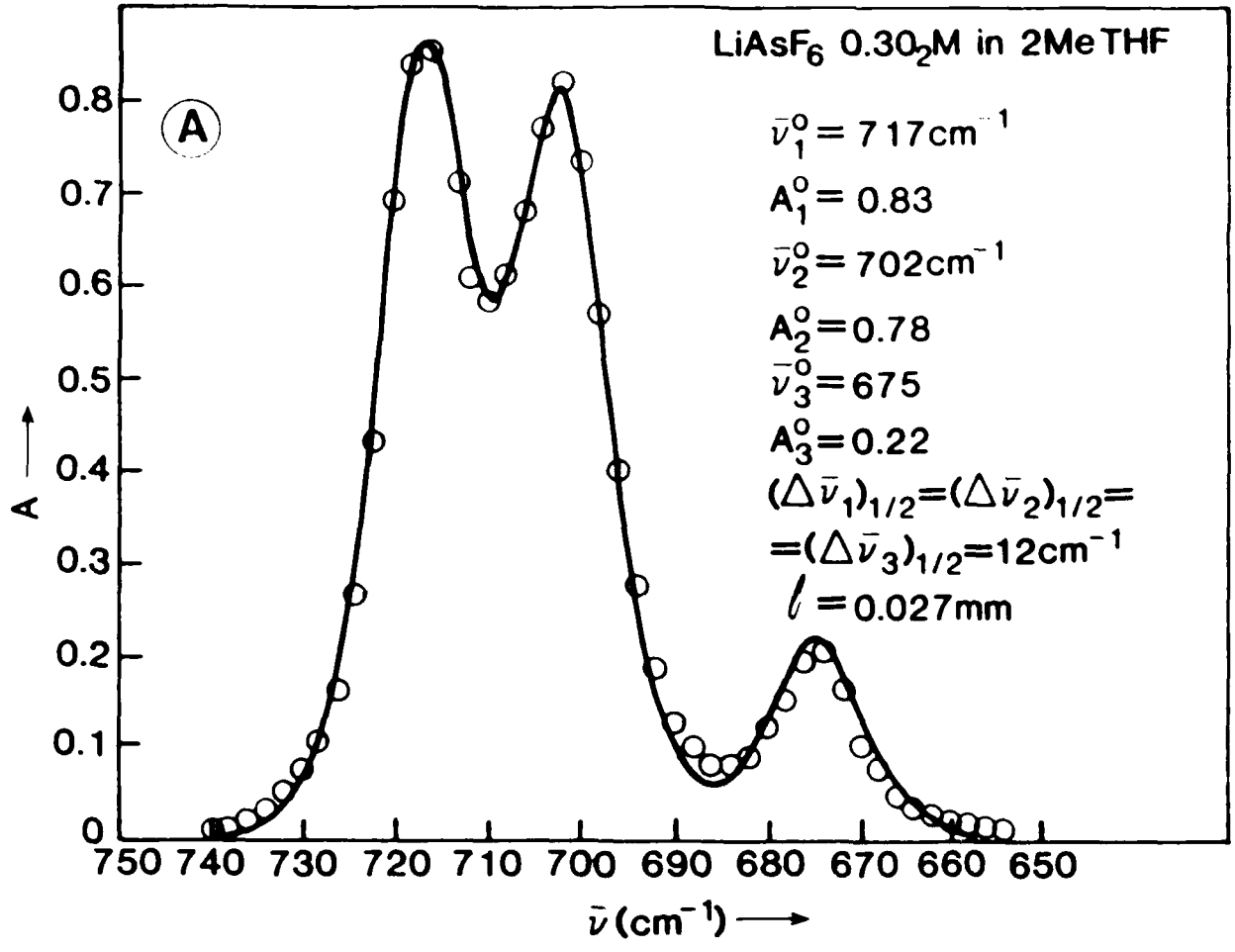
LiAsF6 0.302M in 2MeTHF
A
$\bar{\nu}_1^o = 717 cm^{-1}$
$A_1^o = 0.83$
$\bar{\nu}_2^o = 702 cm^{-1}$
$A_2^o = 0.78$
$\bar{\nu}_3^o = 675$
$A_3^o = 0.22$
$(\Delta\bar{\nu}_1)_{1/2} = (\Delta\bar{\nu}_2)_{1/2} = (\Delta\bar{\nu}_3)_{1/2} = 12 cm^{-1}$
$\ell = 0.027 mm$
A
0.8
0.7
0.6
0.5
0.4
0.3
0.2
0.1
0
750 740 730 720 710 700 690 680 670 660 650
$\bar{\nu}\,(cm^{-1}) \longrightarrow$

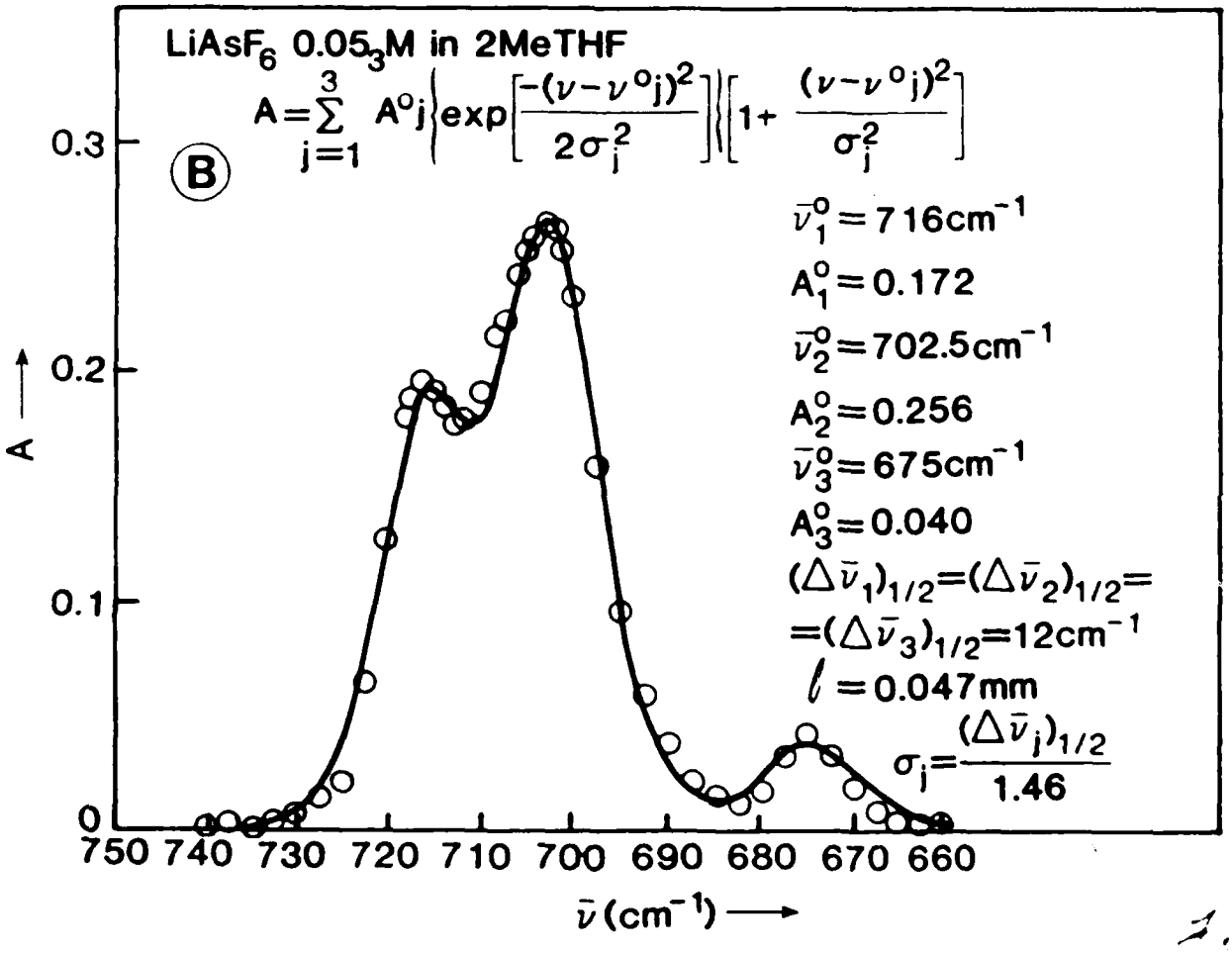
LiAsF6 0.053M in 2MeTHF
$A = \sum_{j=1}^{3} A^o_j \left\{ \exp\left[\frac{-(\nu-\nu^o j)^2}{2\sigma_j^2}\right] \right\} \left[1 + \frac{(\nu-\nu^o j)^2}{\sigma_j^2}\right]$
B
$\bar{\nu}_1^o = 716 cm^{-1}$
$A_1^o = 0.172$
$\bar{\nu}_2^o = 702.5 cm^{-1}$
$A_2^o = 0.256$
$\bar{\nu}_3^o = 675 cm^{-1}$
$A_3^o = 0.040$
$(\Delta\bar{\nu}_1)_{1/2} = (\Delta\bar{\nu}_2)_{1/2} = (\Delta\bar{\nu}_3)_{1/2} = 12 cm^{-1}$
$\ell = 0.047 mm$
$\sigma_j = \frac{(\Delta\bar{\nu}_j)_{1/2}}{1.46}$
A
0.3
0.2
0.1
0
750 740 730 720 710 700 690 680 670 660
$\bar{\nu}\,(cm^{-1}) \longrightarrow$

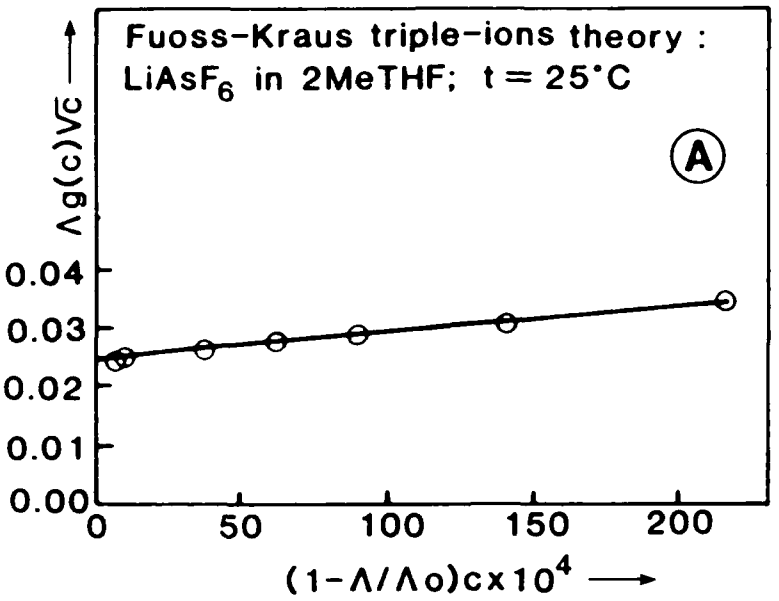
Fuoss-Kraus triple-ions theory :
LiAsF6 in 2MeTHF; t = 25°C
A
Λg(c)√c
0.04
0.03
0.02
0.01
0.00
0
50
100
150
200
(1-Λ/Λo)cx10^4

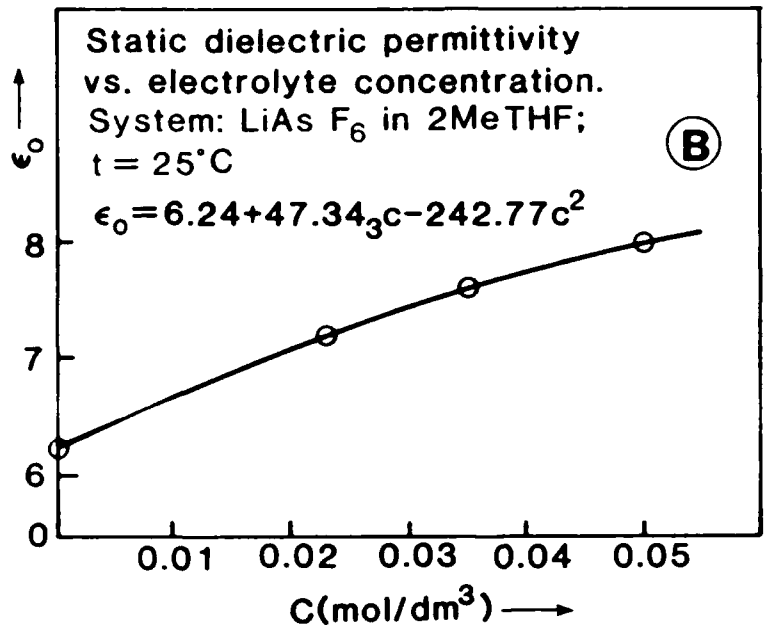
Static dielectric permittivity
vs. electrolyte concentration.
System: LiAs F6 in 2MeTHF;
t = 25°C
ϵo=6.24+47.34₃c-242.77c²
B
ϵo
8
7
6
0
0.01
0.02
0.03
0.04
0.05
C(mol/dm³)

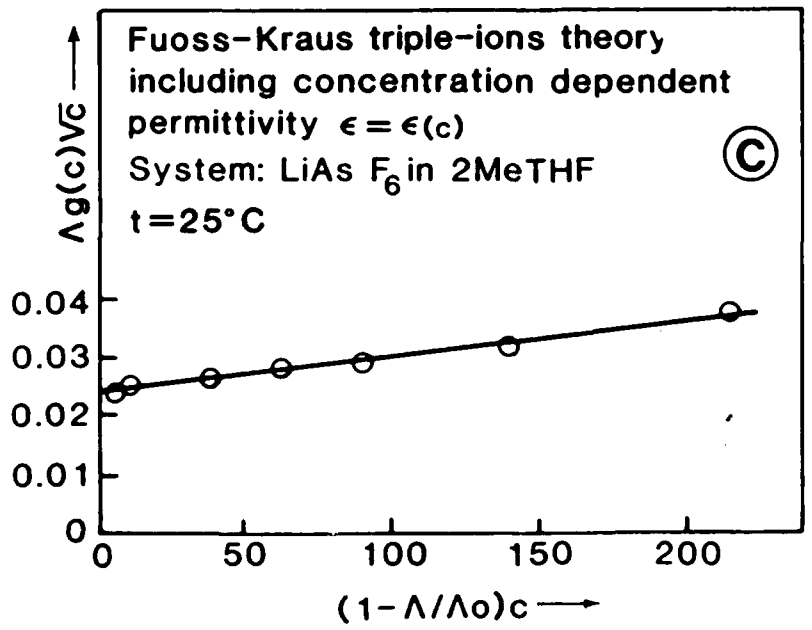
Fuoss-Kraus triple-ions theory
including concentration dependent
permittivity ϵ = ϵ(c)
System: LiAs F6 in 2MeTHF
t=25°C
C
Λg(c)√c
0.04
0.03
0.02
0.01
0
0
50
100
150
200
(1-Λ/Λo)c

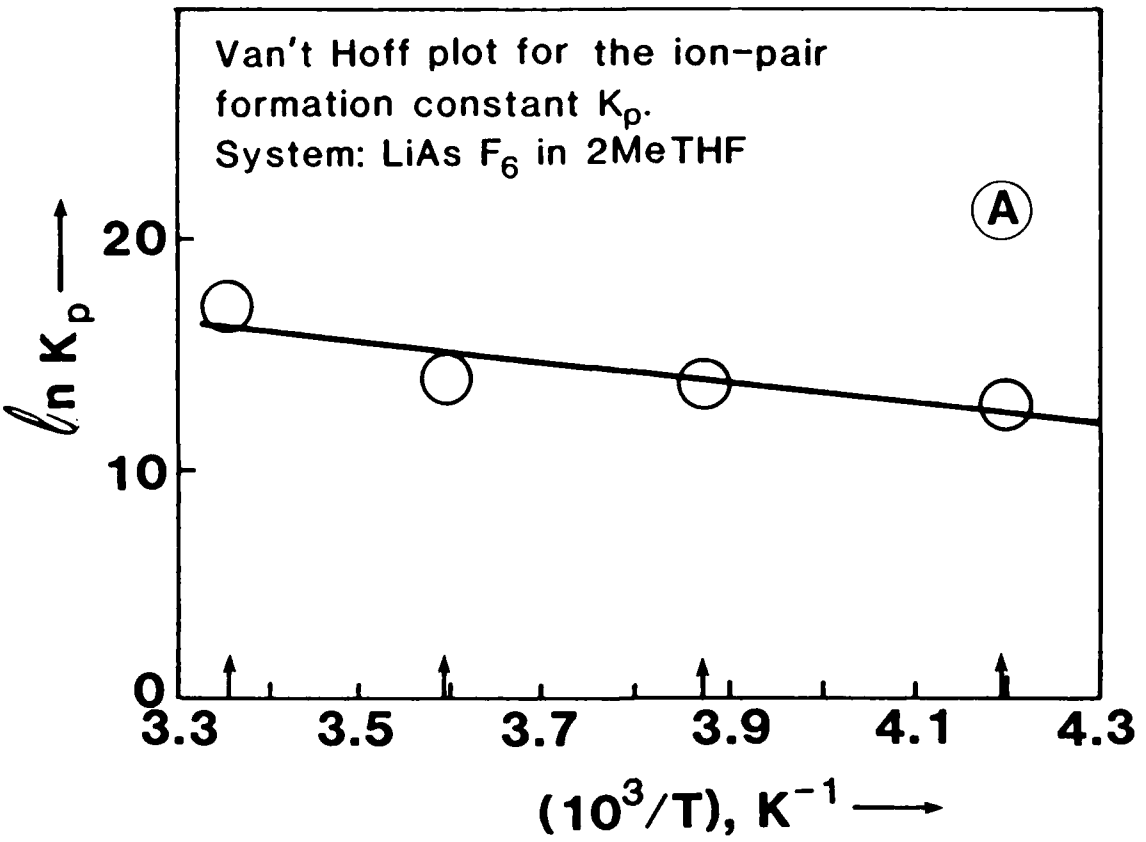
Van't Hoff plot for the ion-pair formation constant K_p.
System: LiAs F_6 in 2MeTHF
A
$\ln K_p$
20
10
0
3.3
3.5
3.7
3.9
4.1
4.3
$(10^3/T)$, K^{-1}

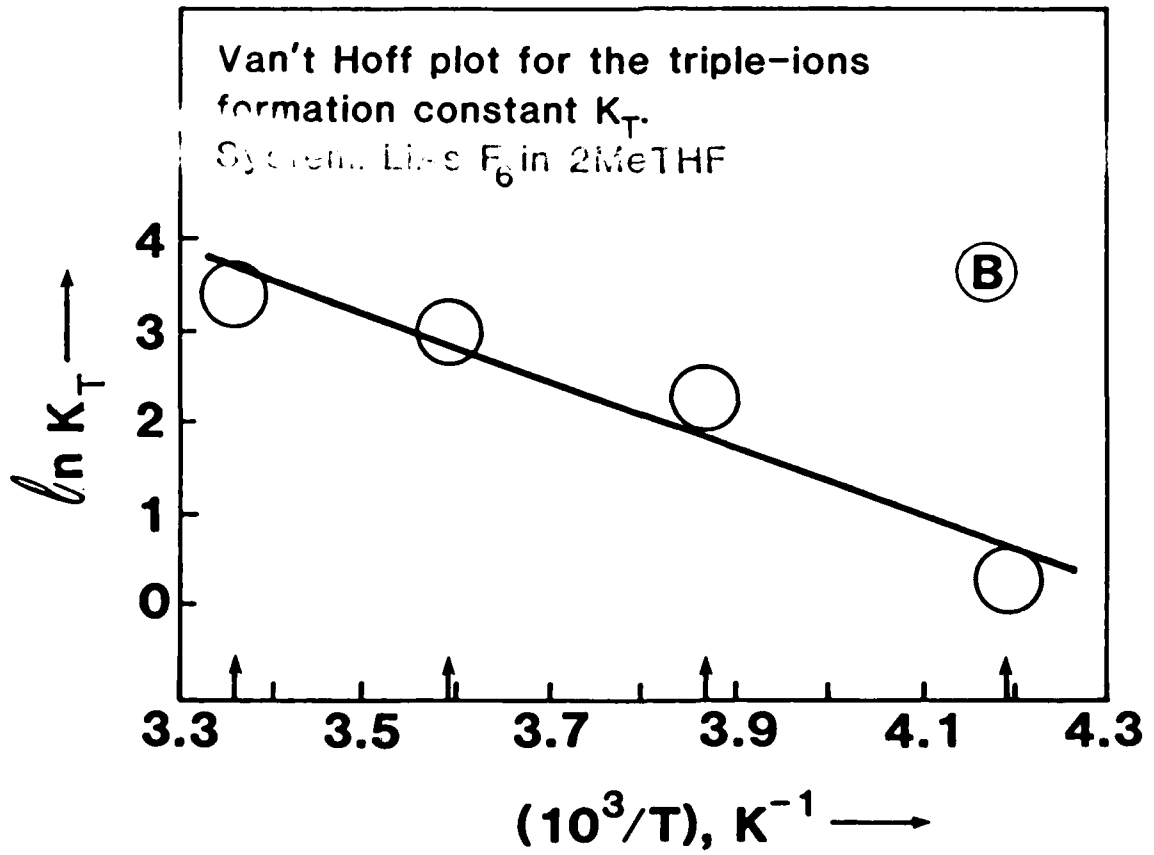
Van't Hoff plot for the triple-ions formation constant K_T.
System: LiAs F_6 in 2MeTHF
B
$\ln K_T$
4
3
2
1
0
3.3
3.5
3.7
3.9
4.1
4.3
$(10^3/T)$, K^{-1}

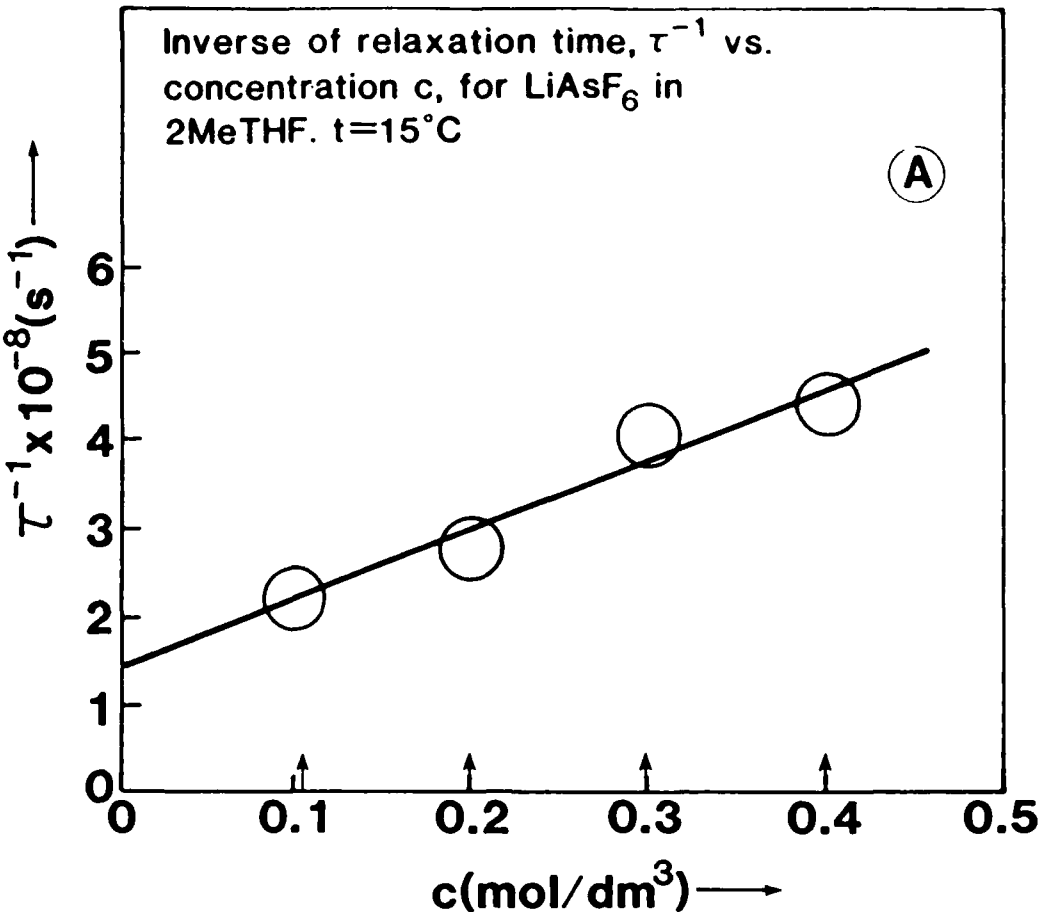
Inverse of relaxation time, τ^{-1} vs. concentration c, for $LiAsF_6$ in 2MeTHF. t=15°C
A
$\tau^{-1} \times 10^{-8}(s^{-1})$
0
1
2
3
4
5
6
0
0.1
0.2
0.3
0.4
0.5
$c(mol/dm^3)$

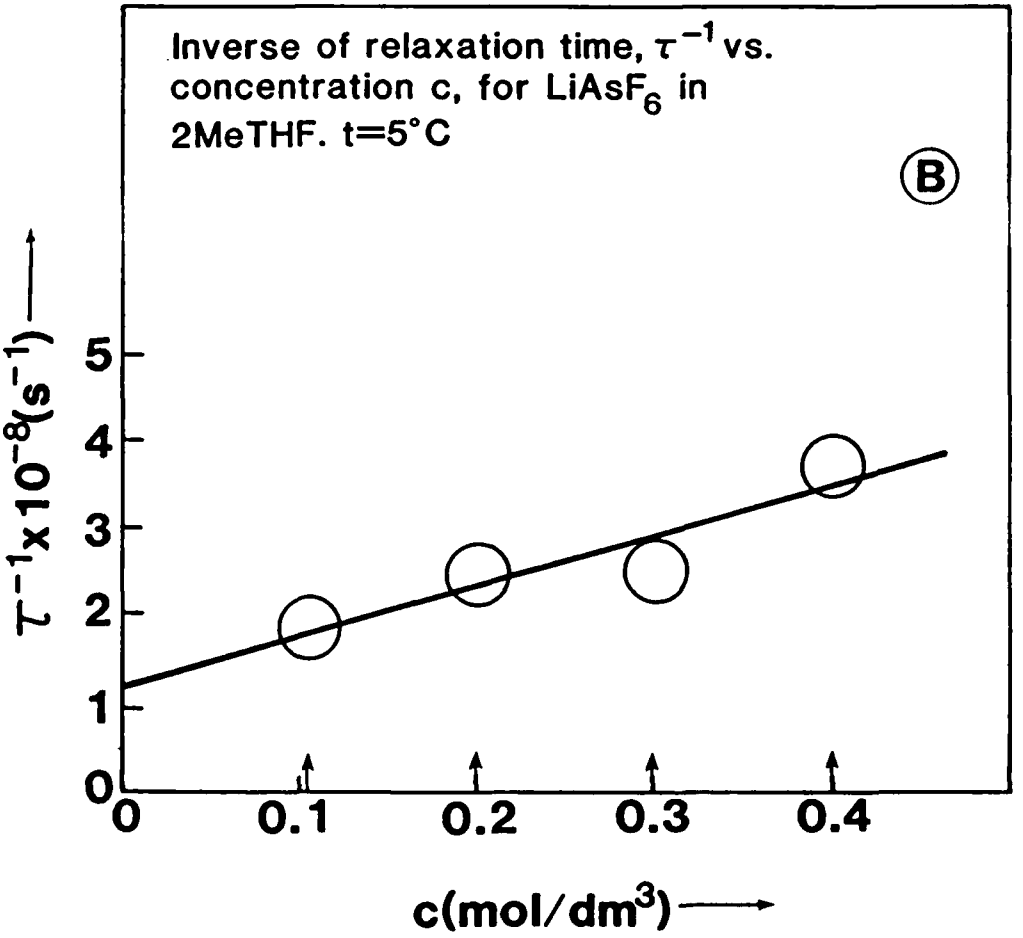
Inverse of relaxation time, τ^{-1} vs. concentration c, for $LiAsF_6$ in 2MeTHF. t=5°C
B
$\tau^{-1} \times 10^{-8}(s^{-1})$
0
1
2
3
4
5
0
0.1
0.2
0.3
0.4
$c(mol/dm^3)$

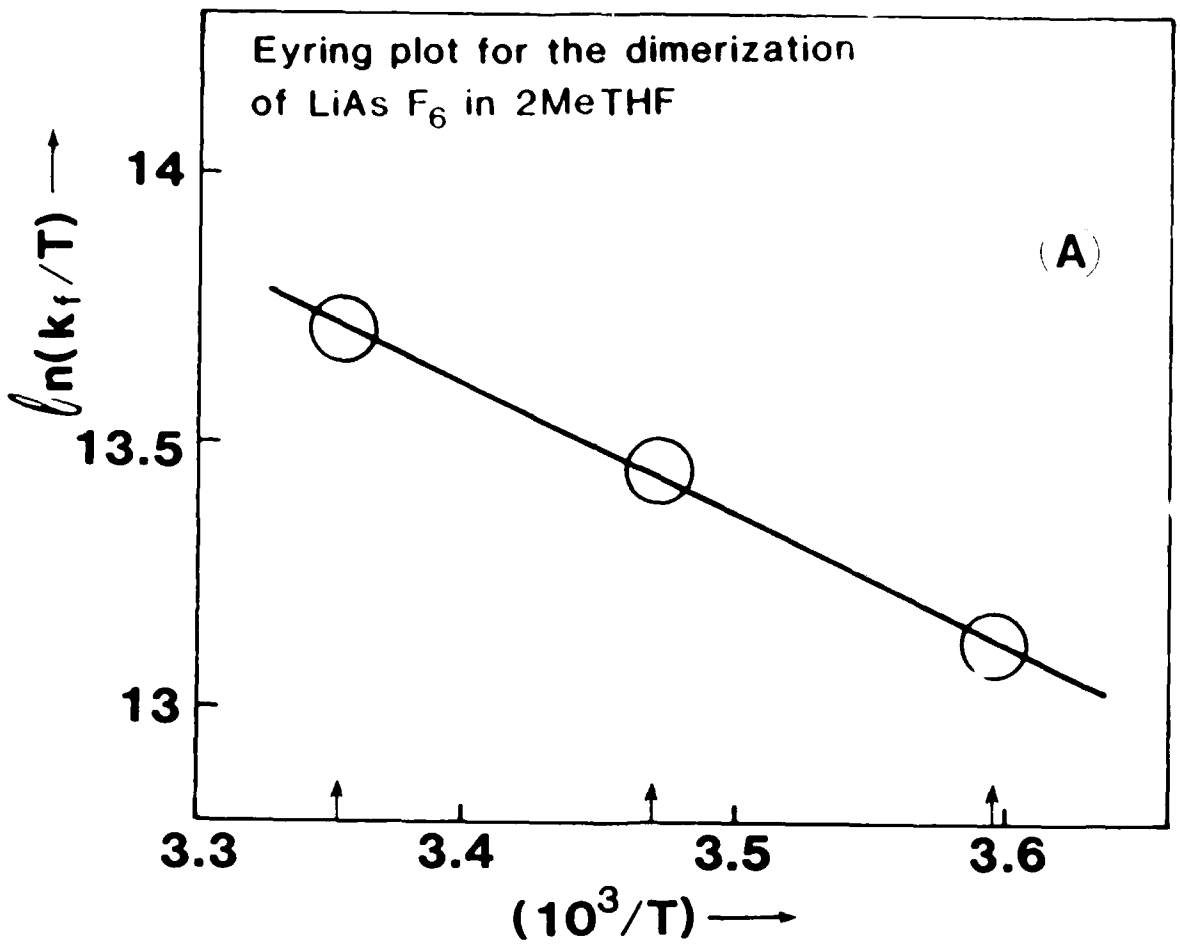
Eyring plot for the dimerization
of LiAs F_6 in 2MeTHF
$\ln(k_f/T)$ ⟶
14
13.5
13
(A)
3.3
3.4
3.5
3.6
$(10^3/T)$ ⟶

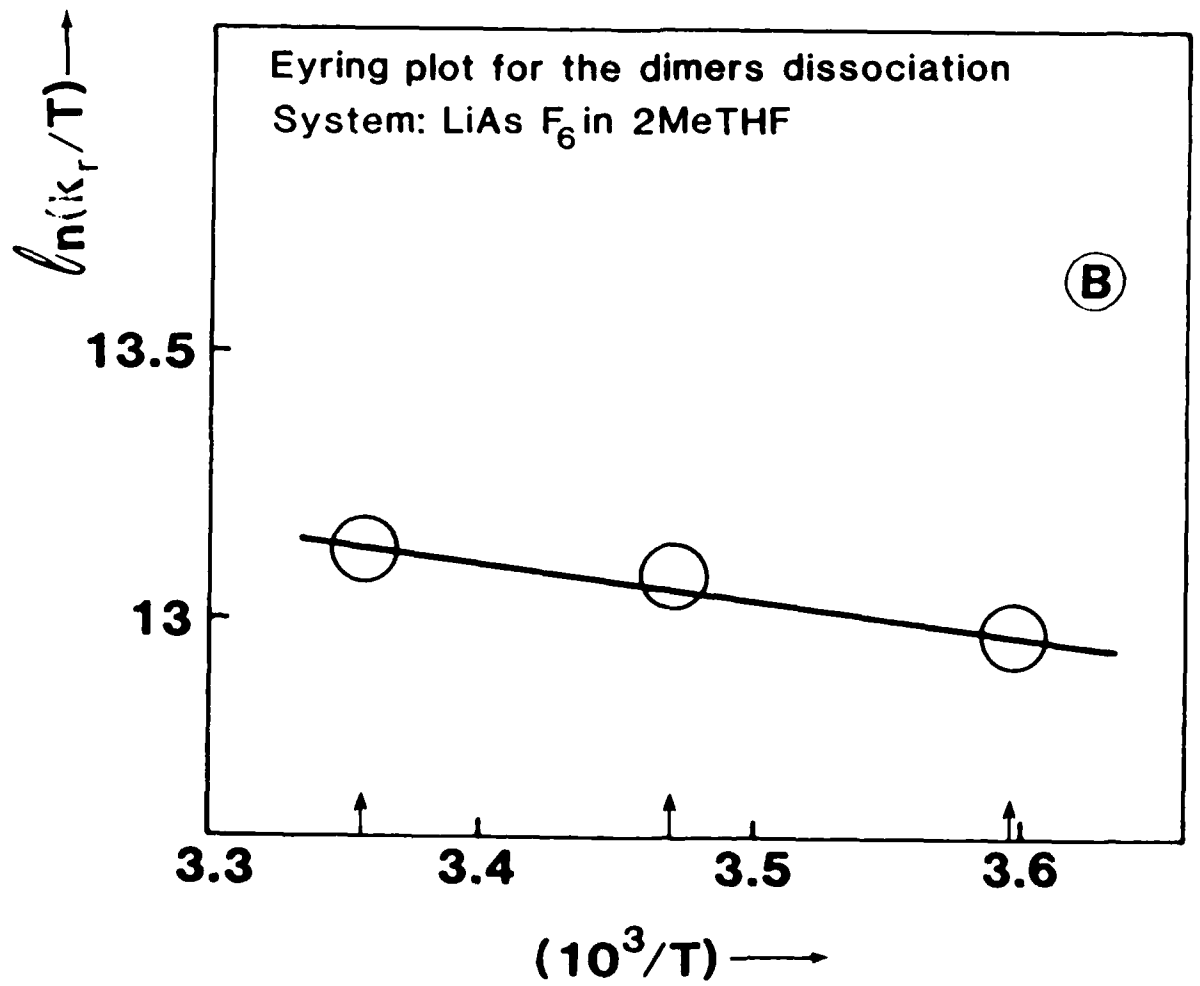
Eyring plot for the dimers dissociation
System: LiAs F_6 in 2MeTHF
$\ln(k_r/T)$ ⟶
13.5
13
(B)
3.3
3.4
3.5
3.6
$(10^3/T)$ ⟶

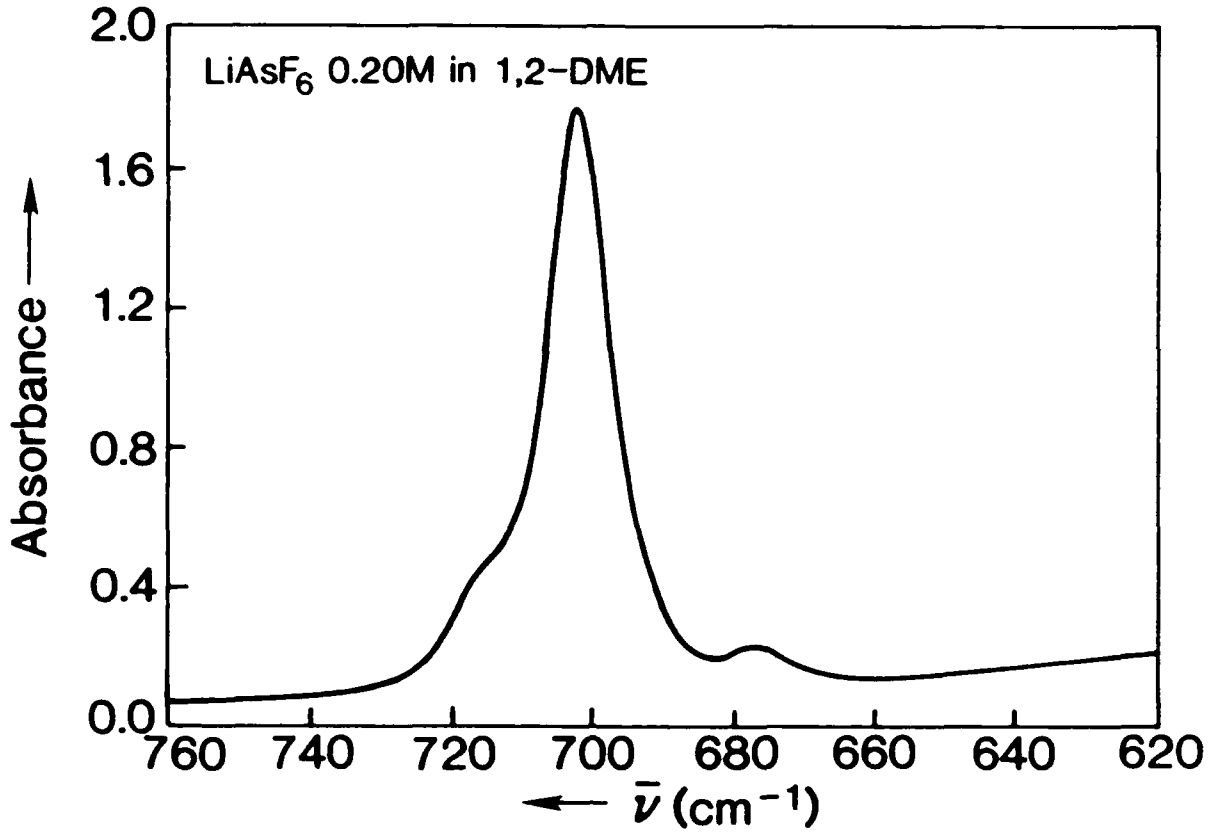
LiAsF6 0.20M in 1,2-DME
Absorbance
2.0
1.6
1.2
0.8
0.4
0.0
760 740 720 700 680 660 640 620
ν̄ (cm⁻¹)

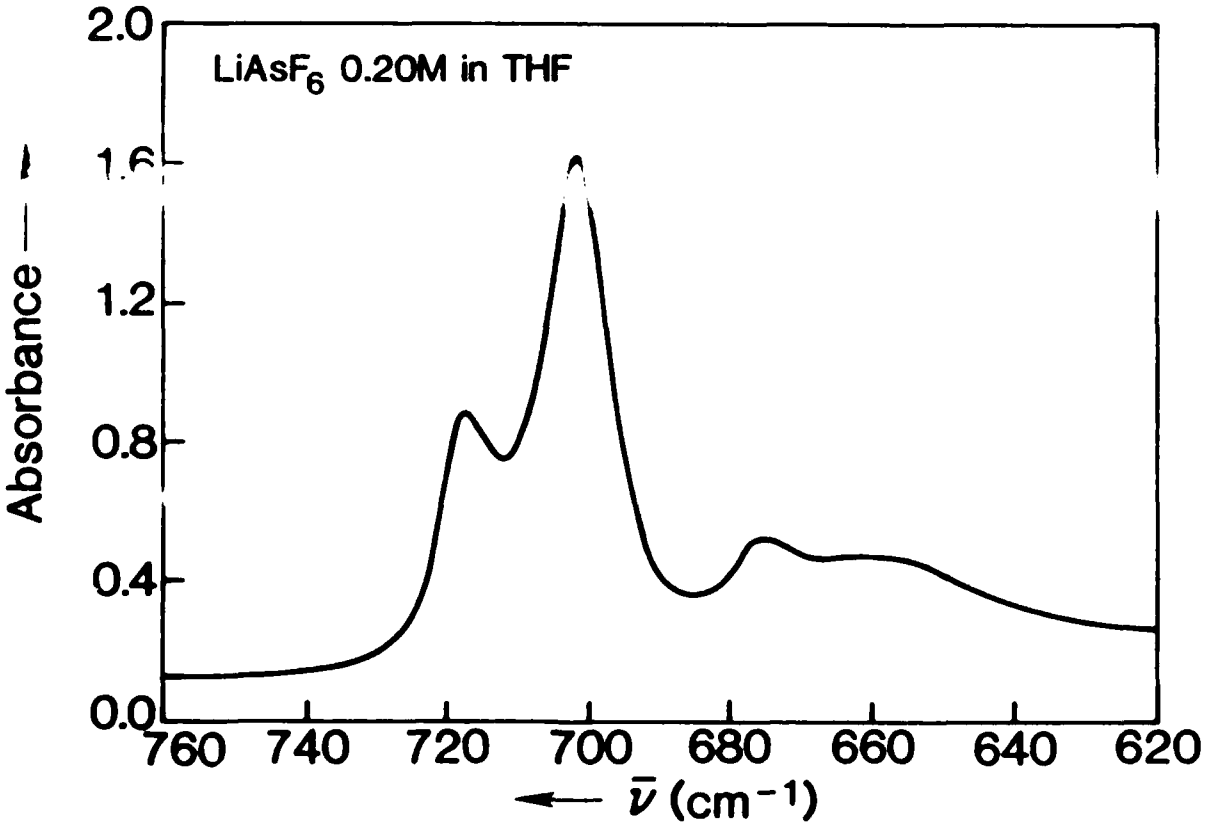
LiAsF6 0.20M in THF
Absorbance
2.0
1.6
1.2
0.8
0.4
0.0
760 740 720 700 680 660 640 620
ν̄ (cm⁻¹)

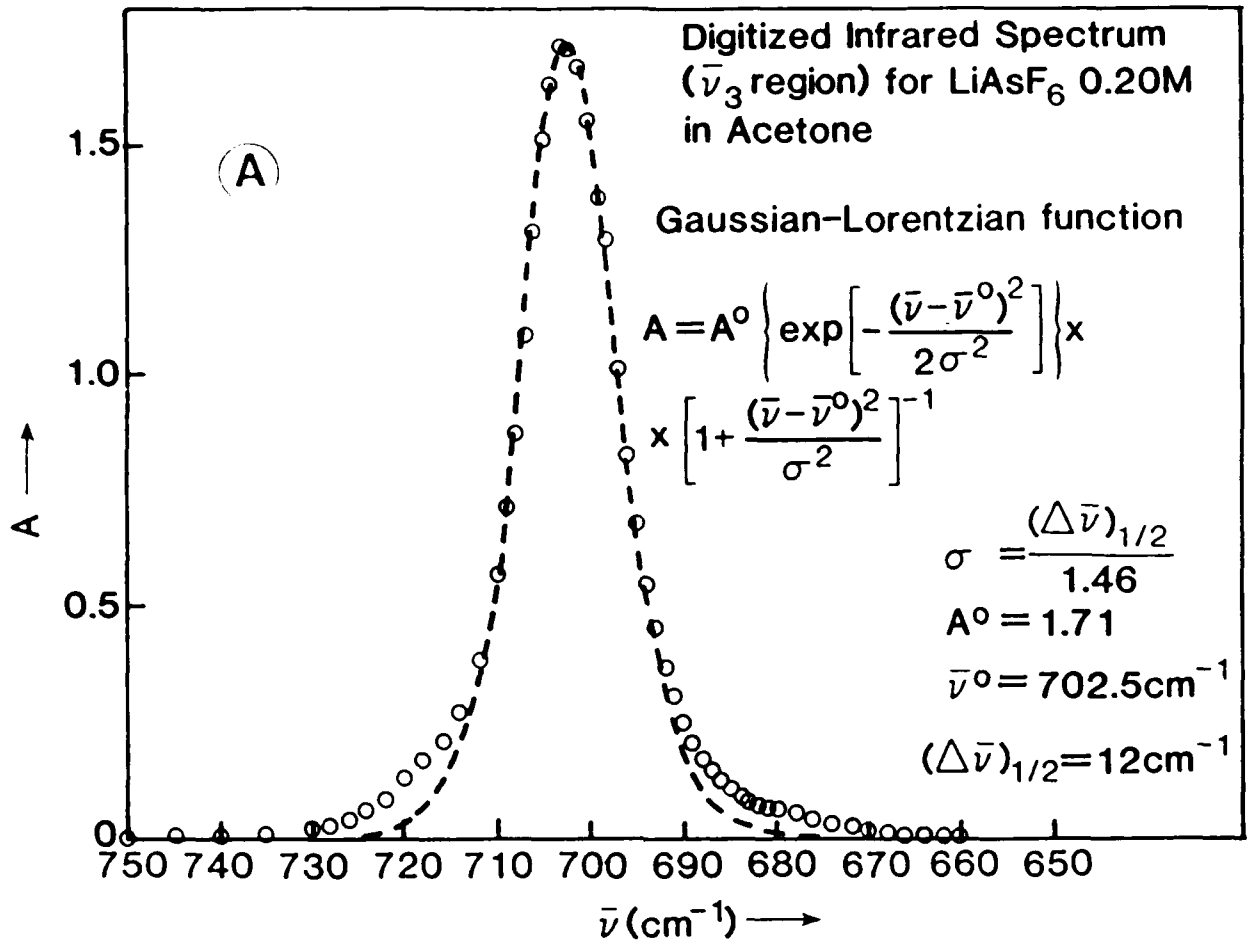
Digitized Infrared Spectrum ($\bar{\nu}_3$ region) for $LiAsF_6$ 0.20M in Acetone
A
Gaussian–Lorentzian function
$A = A^o \left\{ \exp\left[-\frac{(\bar{\nu}-\bar{\nu}^o)^2}{2\sigma^2} \right] \right\} x$
$x \left[1 + \frac{(\bar{\nu}-\bar{\nu}^o)^2}{\sigma^2} \right]^{-1}$
$\sigma = \frac{(\Delta\bar{\nu})_{1/2}}{1.46}$
$A^o = 1.71$
$\bar{\nu}^o = 702.5 cm^{-1}$
$(\Delta\bar{\nu})_{1/2} = 12 cm^{-1}$
A
1.5
1.0
0.5
0
750 740 730 720 710 700 690 680 670 660 650
$\bar{\nu}\,(cm^{-1}) \longrightarrow$

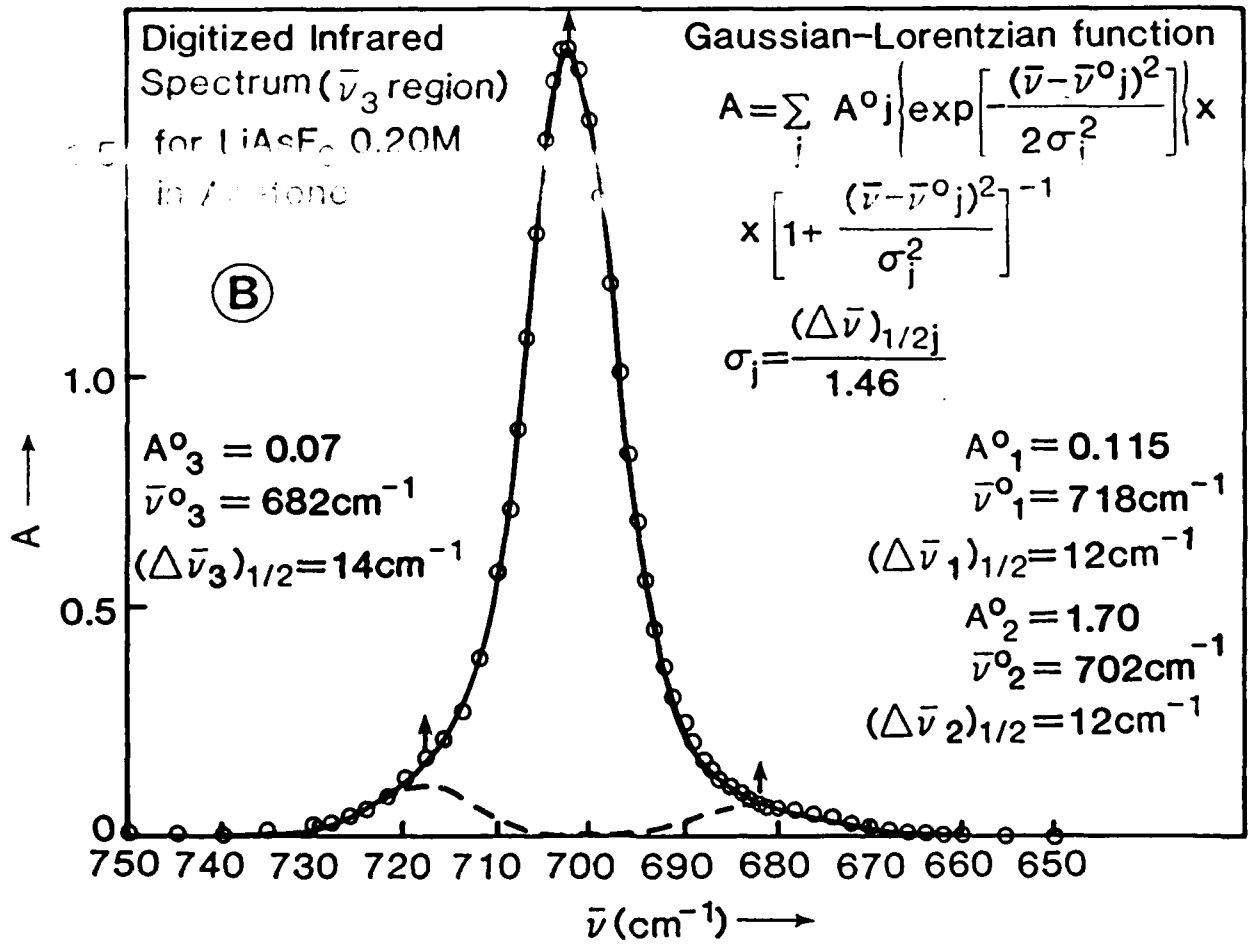
Digitized Infrared Spectrum ($\bar{\nu}_3$ region) for LiAsF6 0.20M in Acetone
B
Gaussian–Lorentzian function
$A = \sum_j A^o j \left\{ \exp\left[-\frac{(\bar{\nu}-\bar{\nu}^o j)^2}{2\sigma_j^2} \right] \right\} x$
$x \left[1 + \frac{(\bar{\nu}-\bar{\nu}^o j)^2}{\sigma_j^2} \right]^{-1}$
$\sigma_j = \frac{(\Delta\bar{\nu})_{1/2j}}{1.46}$
$A^o_3 = 0.07$
$\bar{\nu}^o_3 = 682 cm^{-1}$
$(\Delta\bar{\nu}_3)_{1/2} = 14 cm^{-1}$
$A^o_1 = 0.115$
$\bar{\nu}^o_1 = 718 cm^{-1}$
$(\Delta\bar{\nu}_1)_{1/2} = 12 cm^{-1}$
$A^o_2 = 1.70$
$\bar{\nu}^o_2 = 702 cm^{-1}$
$(\Delta\bar{\nu}_2)_{1/2} = 12 cm^{-1}$
A
1.0
0.5
0
750 740 730 720 710 700 690 680 670 660 650
$\bar{\nu}\,(cm^{-1}) \longrightarrow$

Fig. 9

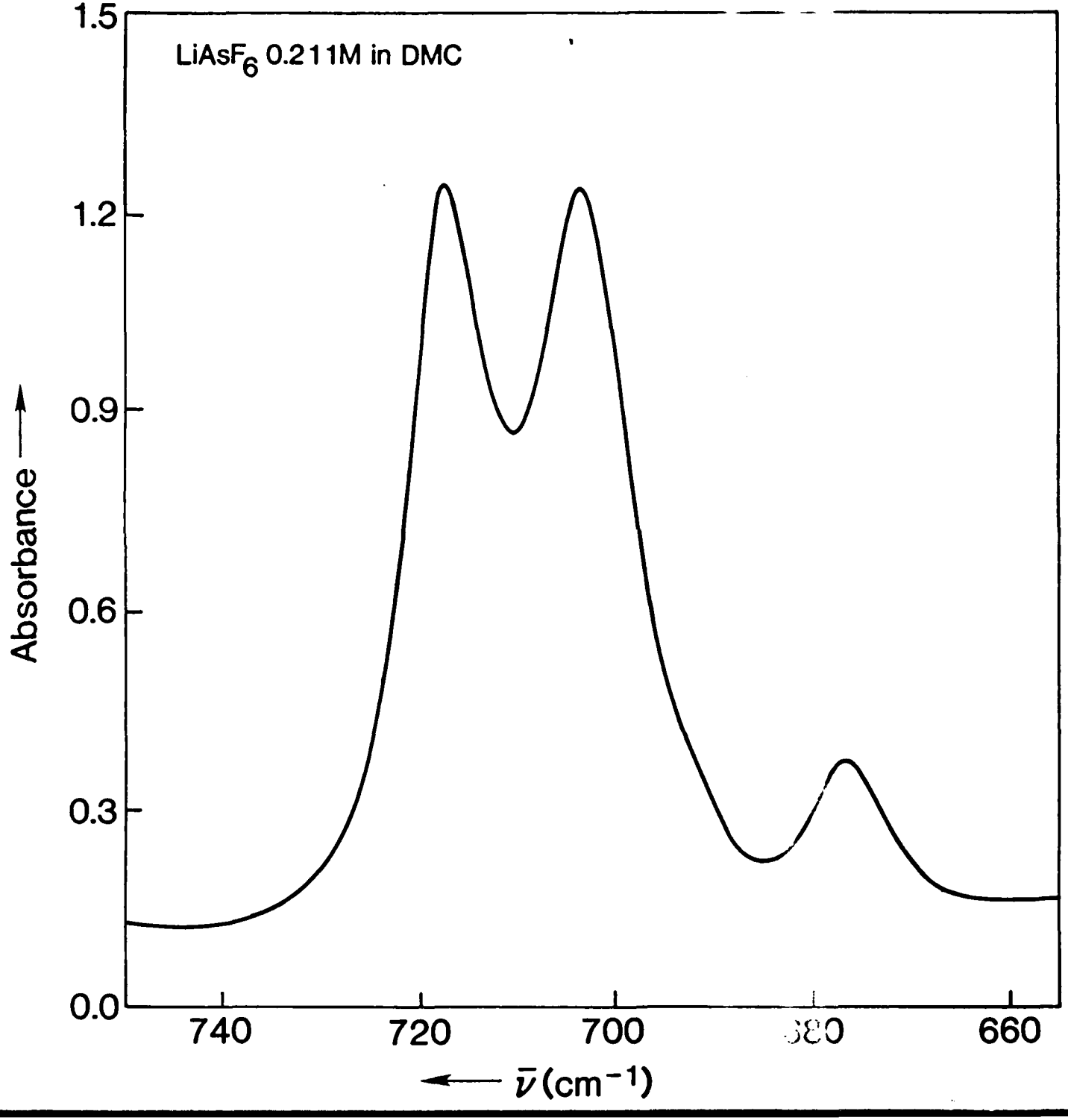
LiAsF6 0.211M in DMC
1.5
1.2
0.9
0.6
0.3
0.0
Absorbance
740
720
700
660
ν̄ (cm⁻¹)

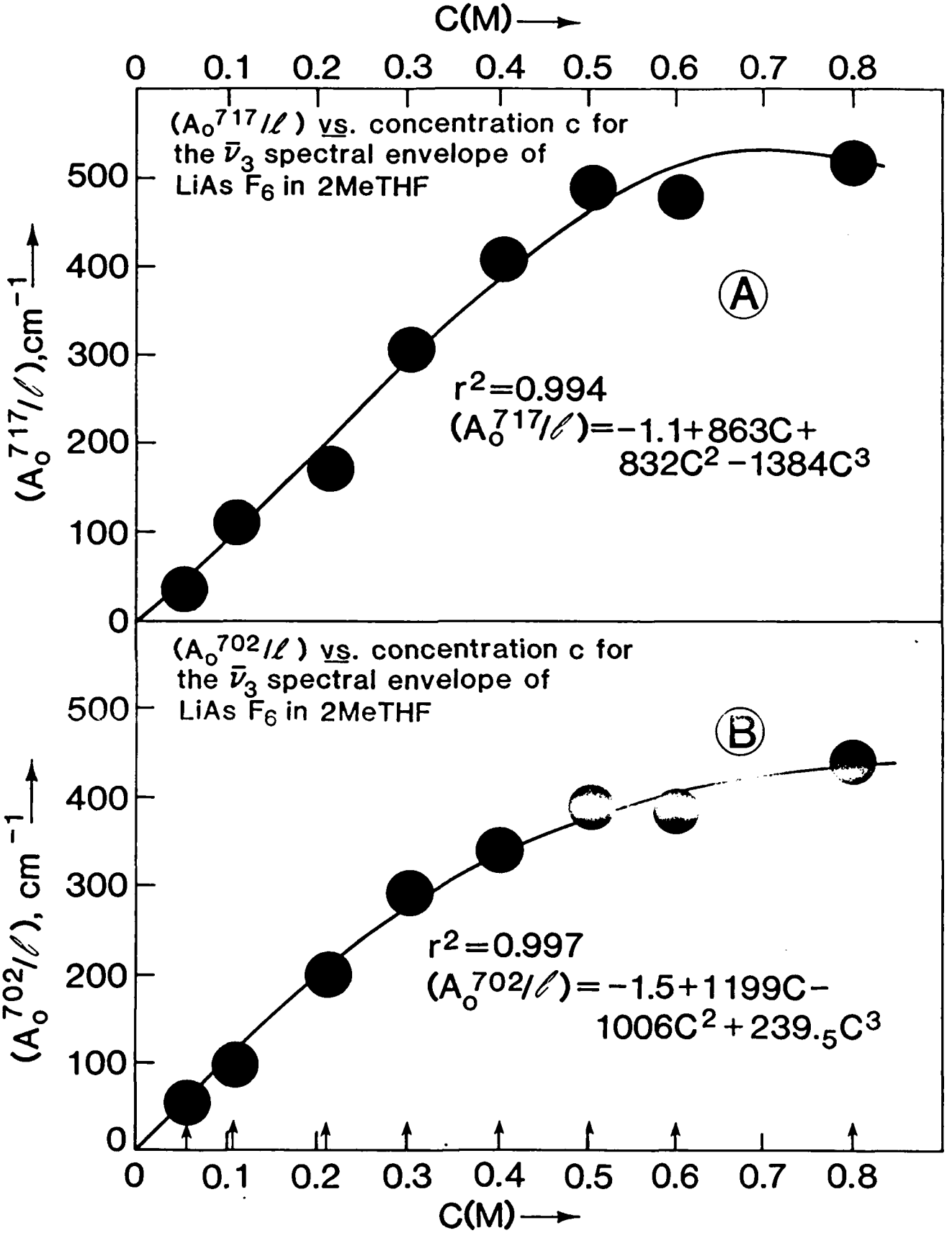
C(M) →
0 0.1 0.2 0.3 0.4 0.5 0.6 0.7 0.8
(A_o^{717}/ℓ) vs. concentration c for the $\bar{\nu}_3$ spectral envelope of LiAs F_6 in 2MeTHF
(A_o^{717}/ℓ),cm^{-1} →
500
400
300
200
100
0
A
r^2=0.994
(A_o^{717}/ℓ)=−1.1+863C+ 832C^2 −1384C^3
(A_o^{702}/ℓ) vs. concentration c for the $\bar{\nu}_3$ spectral envelope of LiAs F_6 in 2MeTHF
(A_o^{702}/ℓ), cm^{-1} →
B
r^2=0.997
(A_o^{702}/ℓ)=−1.5+1199C− 1006C^2+239.$_5C^3$
0 0.1 0.2 0.3 0.4 0.5 0.6 0.7 0.8
C(M) →

END

2-87

DTIC